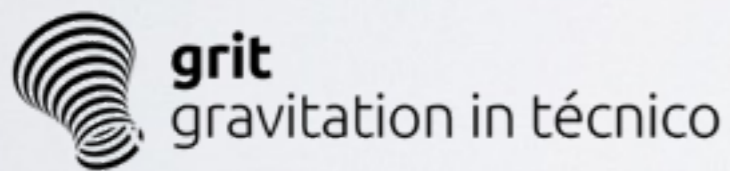
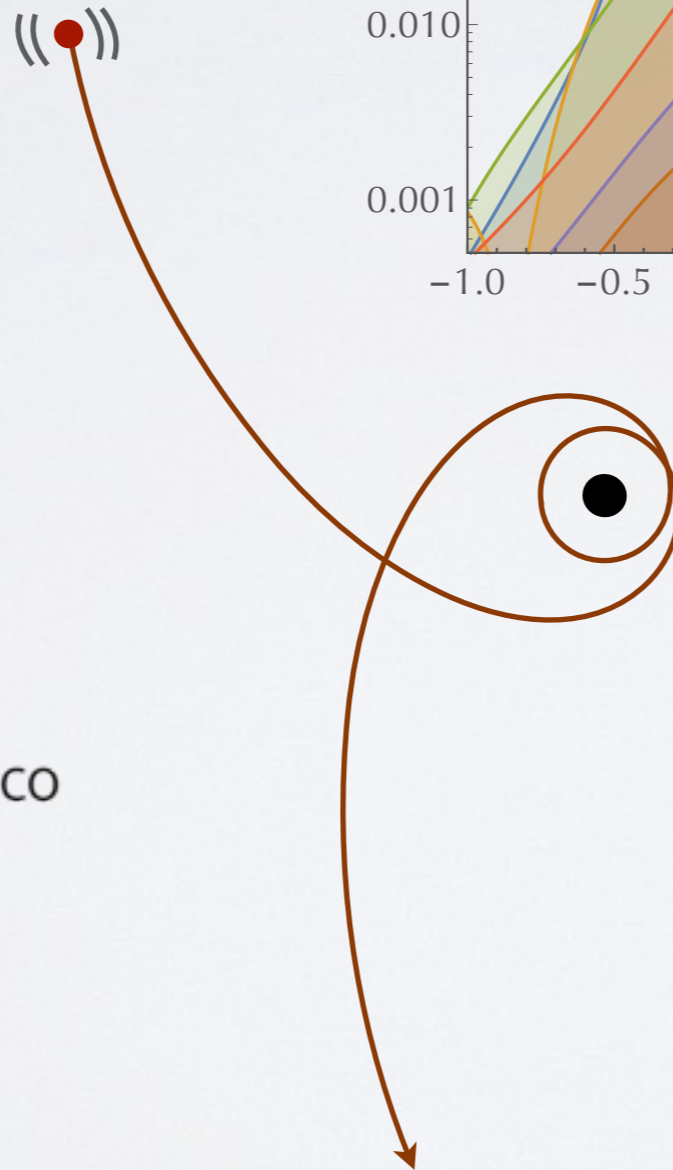
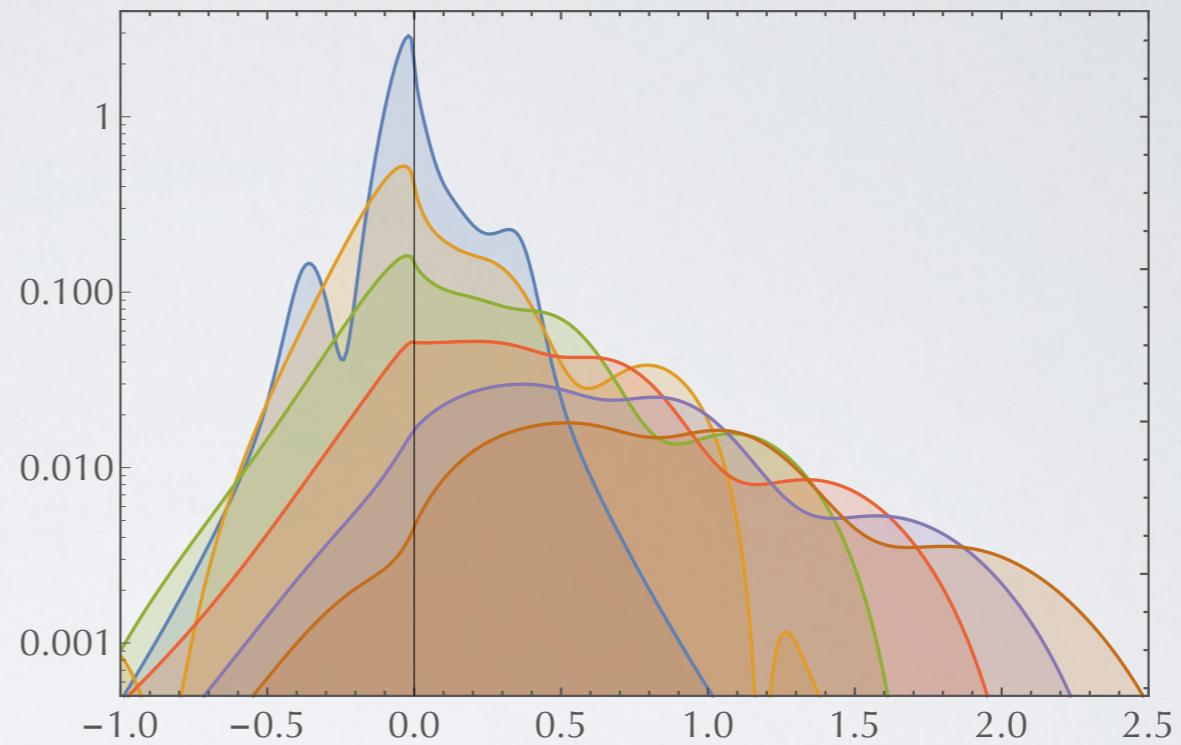


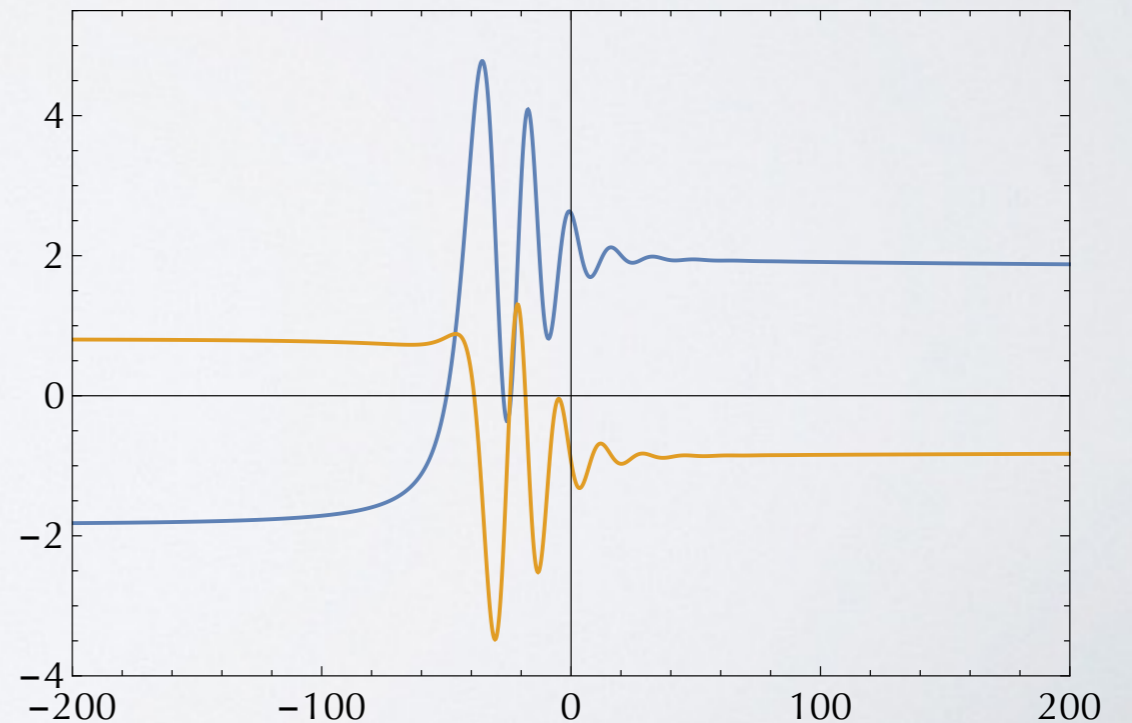
Scattering trajectories in Schwarzschild spacetime

Seth Hopper

Vitor Cardoso



Capra - June 19, 2017

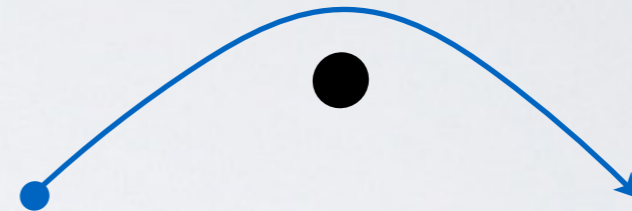


Outline

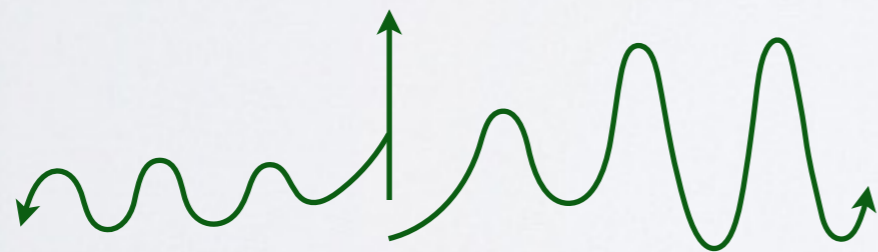
Bound motion



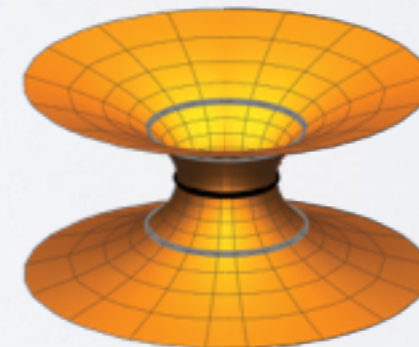
Unbound motion



Local calculations



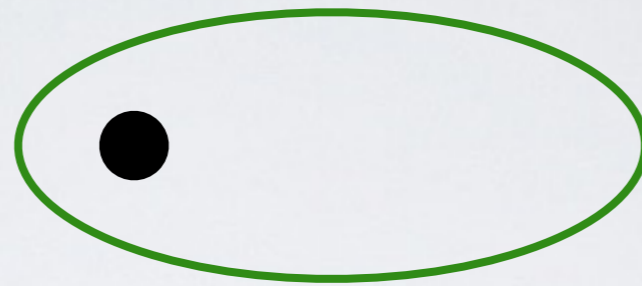
Wormholes and echoes



Peters & Mathews computed the PN flux from bound eccentric motion



Peters & Mathews, 1963



$$\left\langle \frac{dE}{dt} \right\rangle_{3\text{PN}} = \frac{32}{5} \left(\frac{\mu}{M} \right)^2 x^5 \left(\mathcal{I}_0 + x \mathcal{I}_1 + x^{3/2} \mathcal{K}_{3/2} + x^2 \mathcal{I}_2 + x^{5/2} \mathcal{K}_{5/2} + x^3 \mathcal{I}_3 + x^3 \mathcal{K}_3 \right)$$

$$\mathcal{I}_0 = \frac{1}{(1 - e_t^2)^{7/2}} \left(1 + \frac{73}{24} e_t^2 + \frac{37}{96} e_t^4 \right)$$

“Enhances” flux from Hulse-Taylor pulsar ($e=0.62$) by factor of 12

We work in a gauge which simplifies the field equations

Key assumptions

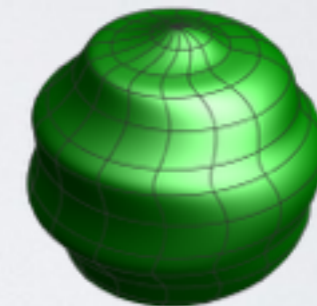
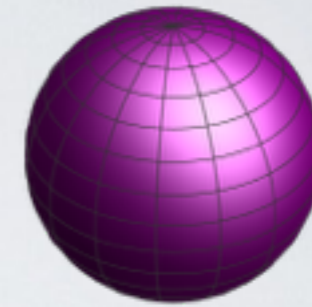
1. Black hole background:

$$g_{\mu\nu}^{\text{BG}} = g_{\mu\nu}^{\text{BH}}$$

2. Small deviations:

$$g_{\mu\nu} = g_{\mu\nu}^{\text{BH}} + h_{\mu\nu} \quad |h_{\mu\nu}| \ll |g_{\mu\nu}^{\text{BH}}|$$

Schwarzschild metric



Metric perturbation

Result

Lorenz gauge:

$$\square \bar{h}_{\mu\nu} + 2R_{\alpha\mu\beta\nu} \bar{h}^{\alpha\beta} = -16\pi T_{\mu\nu}$$

Regge-Wheeler gauge:

$$\left[-\frac{\partial^2}{\partial t^2} + \frac{\partial^2}{\partial r_*^2} - V_\ell(r) \right] \Psi_{\ell m}(t, r) \\ = G_{\ell m}(t) \delta[r - r_p(t)] + F_{\ell m}(t) \delta'[r - r_p(t)]$$

Periodic motion implies a discrete spectrum

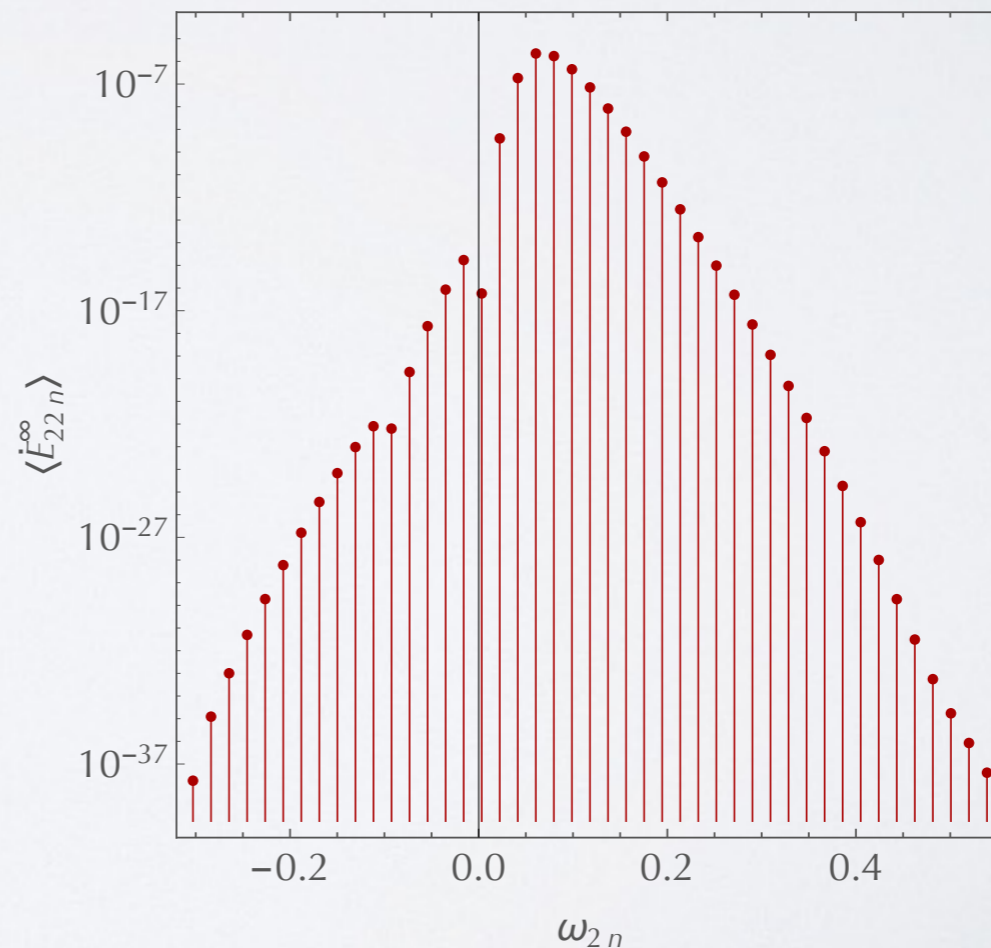


$$\left[-\frac{\partial^2}{\partial t^2} + \frac{\partial^2}{\partial r_*^2} - V_l(r) \right] \Psi_{lm}(t, r) = S_{lm}(t, r) \quad \longrightarrow \quad \left[\frac{d^2}{dr_*^2} + \omega_{mn}^2 - V_l(r) \right] X_{lmn}(r) = Z_{lmn}(r)$$

$$\Psi_{lm}(t, r) = \sum_{n=-\infty}^{\infty} X_{lmn}(r) e^{-i\omega_{mn}t}$$

$$S_{lm}(t, r) = \sum_{n=-\infty}^{\infty} Z_{lmn}(r) e^{-i\omega_{mn}t}$$

$(p, e) = (10, 0.2)$



The particular solution follows from integrating over the source



Time domain

$$\left[-\frac{\partial^2}{\partial t^2} + \frac{\partial^2}{\partial r_*^2} - V_\ell(r) \right] \Psi_{\ell m}(t, r) = \underline{G_{\ell m}(t)} \delta[r - r_p(t)] + \underline{F_{\ell m}(t)} \delta'[r - r_p(t)]$$

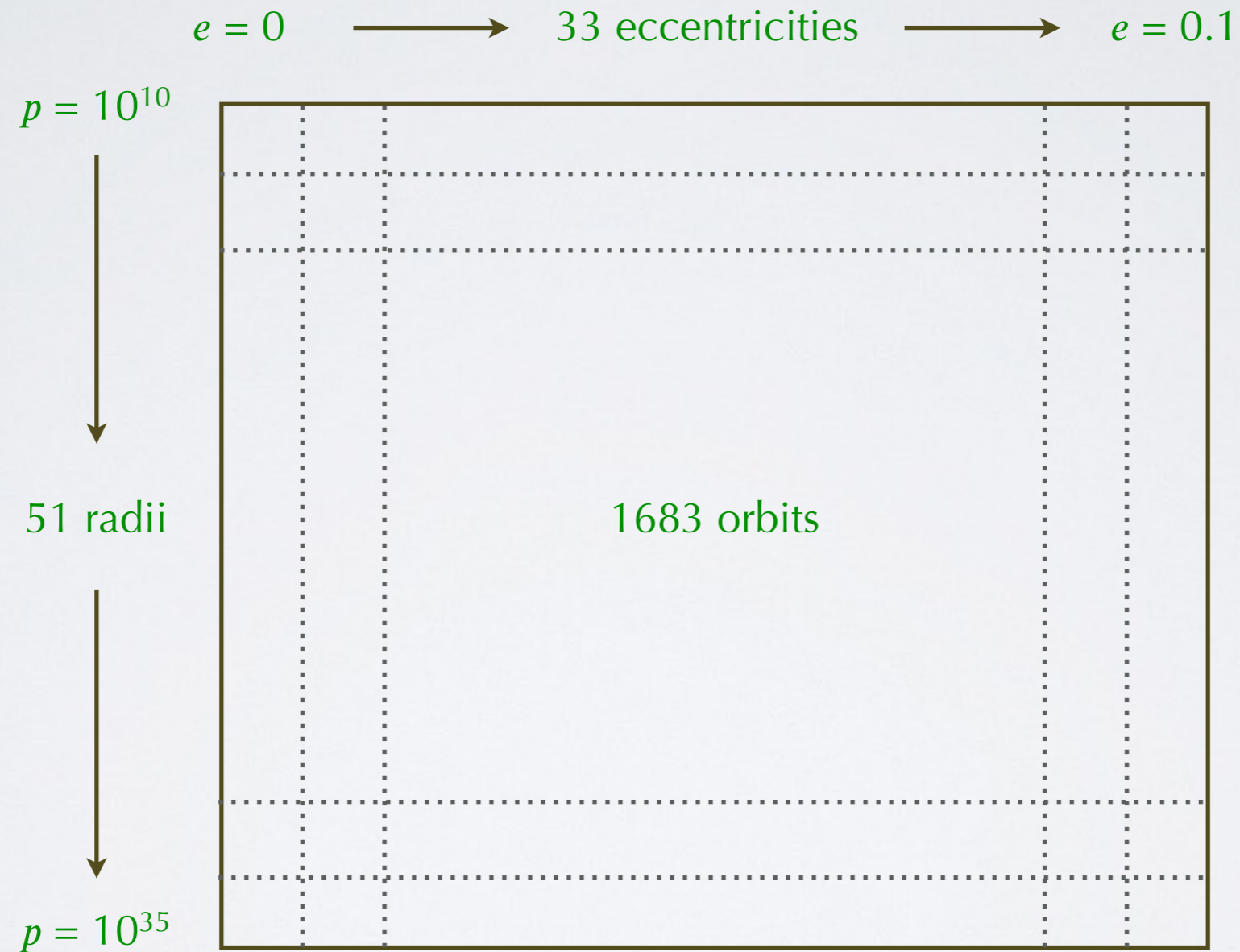
Frequency domain

$$\left[\frac{d^2}{dr_*^2} + \omega^2 - V_\ell(r) \right] X_{\ell m \omega}(r) = Z_{\ell m \omega}(r).$$

$$C_{\ell m \omega}^\pm \sim \int_0^{T_r} dt \left(\hat{X}_{\ell m \omega}^\mp \underline{G_{\ell m}} + \frac{d\hat{X}_{\ell m \omega}^\mp}{dr} \underline{F_{\ell m}} \right)$$

$$\Psi_{\ell m}^\pm(t, r) \equiv \sum_{n=-\infty}^{\infty} C_{\ell m n}^\pm \hat{X}_{\ell m n}^\pm(r) e^{-i\omega_{mn} t}$$

We spanned the two dimensional space of orbits



PN parameters involve sums of transcendentals



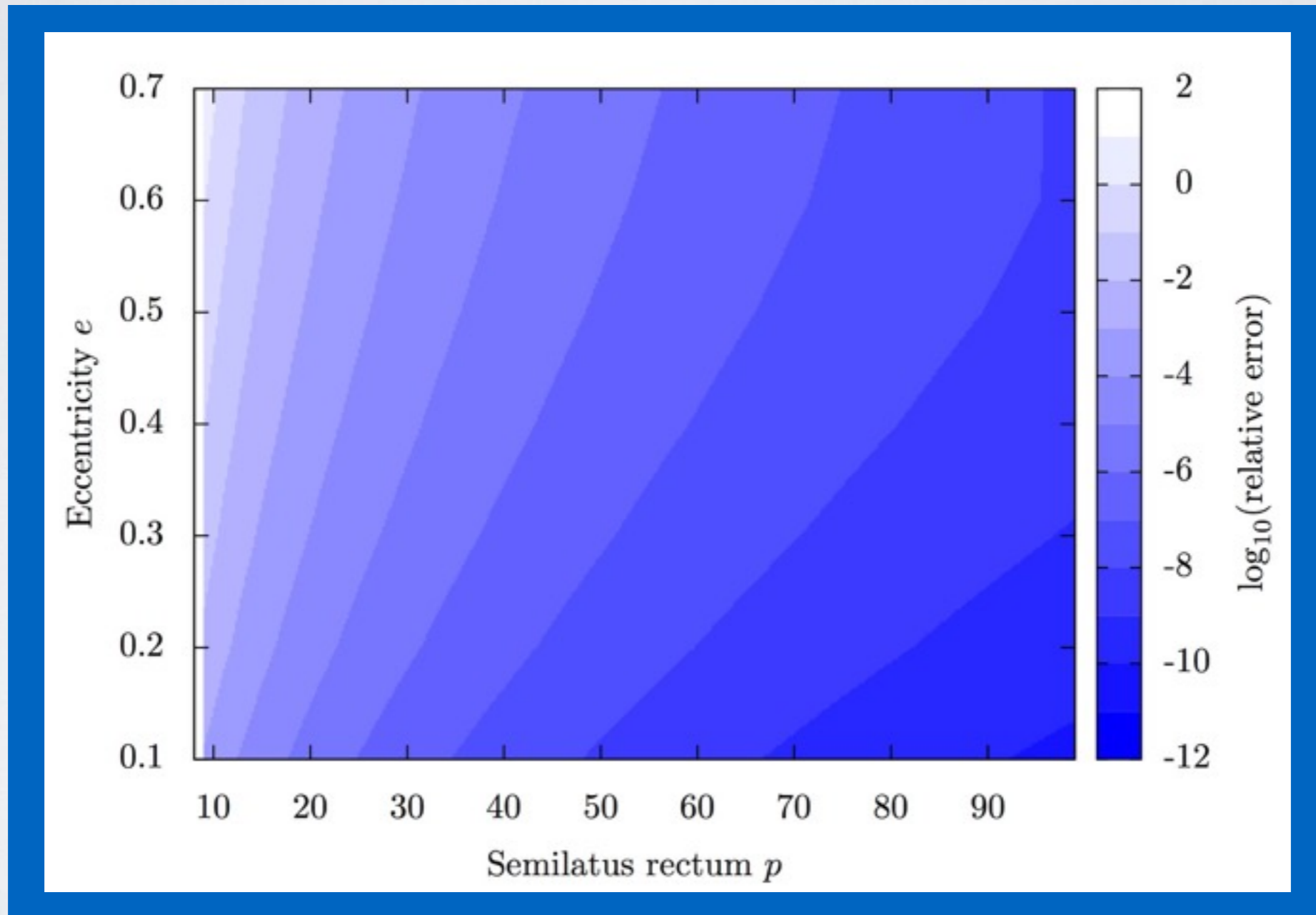
Found with PSLQ algorithm

$$\begin{aligned}
 \mathcal{L}_4 = & \frac{1}{(1 - e^2)^{15/2}} \left[-\frac{323105549467}{3178375200} + \frac{232597}{4410} \gamma_E - \frac{1369}{126} \pi^2 + \frac{39931}{294} \log(2) - \frac{47385}{1568} \log(3) \right. \\
 & + \left(-\frac{128412398137}{23543520} + \frac{4923511}{2940} \gamma_E - \frac{104549}{252} \pi^2 - \frac{343177}{252} \log(2) + \frac{55105839}{15680} \log(3) \right) e^2 \\
 & + \left(-\frac{981480754818517}{25427001600} + \frac{142278179}{17640} \gamma_E - \frac{1113487}{504} \pi^2 + \frac{762077713}{5880} \log(2) - \frac{2595297591}{71680} \log(3) \right. \\
 & \quad \left. - \frac{15869140625}{903168} \log(5) \right) e^4 \\
 & + \left(-\frac{874590390287699}{12713500800} + \frac{318425291}{35280} \gamma_E - \frac{881501}{336} \pi^2 - \frac{90762985321}{63504} \log(2) + \frac{31649037093}{1003520} \log(3) \right. \\
 & \quad \left. + \frac{10089048828125}{16257024} \log(5) \right) e^6 \\
 & + d_8 e^8 + d_{10} e^{10} + d_{12} e^{12} + d_{14} e^{14} + d_{16} e^{16} + d_{18} e^{18} + d_{20} e^{20} + d_{22} e^{22} + d_{24} e^{24} + d_{26} e^{26} \\
 & \left. + d_{28} e^{28} + d_{30} e^{30} + d_{32} e^{32} + d_{34} e^{34} + d_{36} e^{36} + d_{38} e^{38} + d_{40} e^{40} + \dots \right]
 \end{aligned}$$

New PN parameters have been confirmed with a separate code



Flux residuals after subtracting new PN parameters



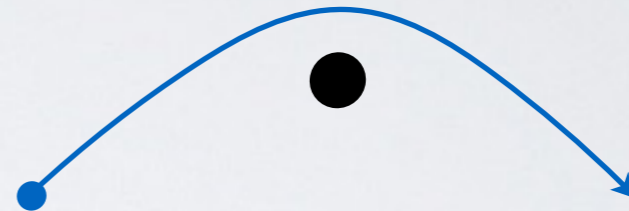
Code by Thomas Osburn

Outline

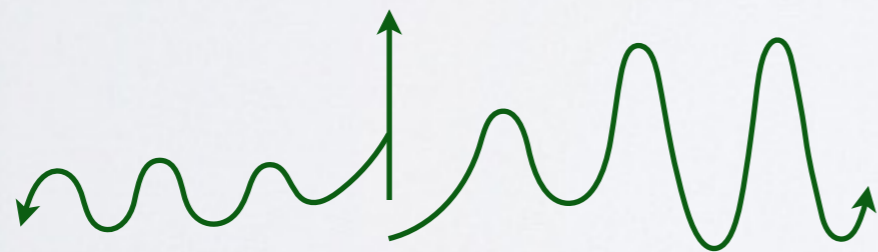
Bound motion



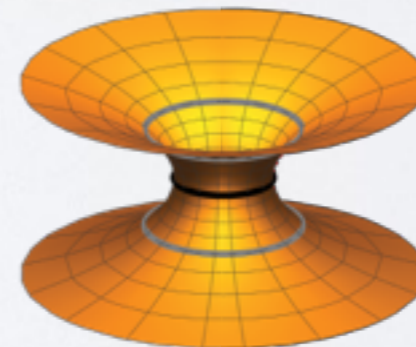
Unbound motion



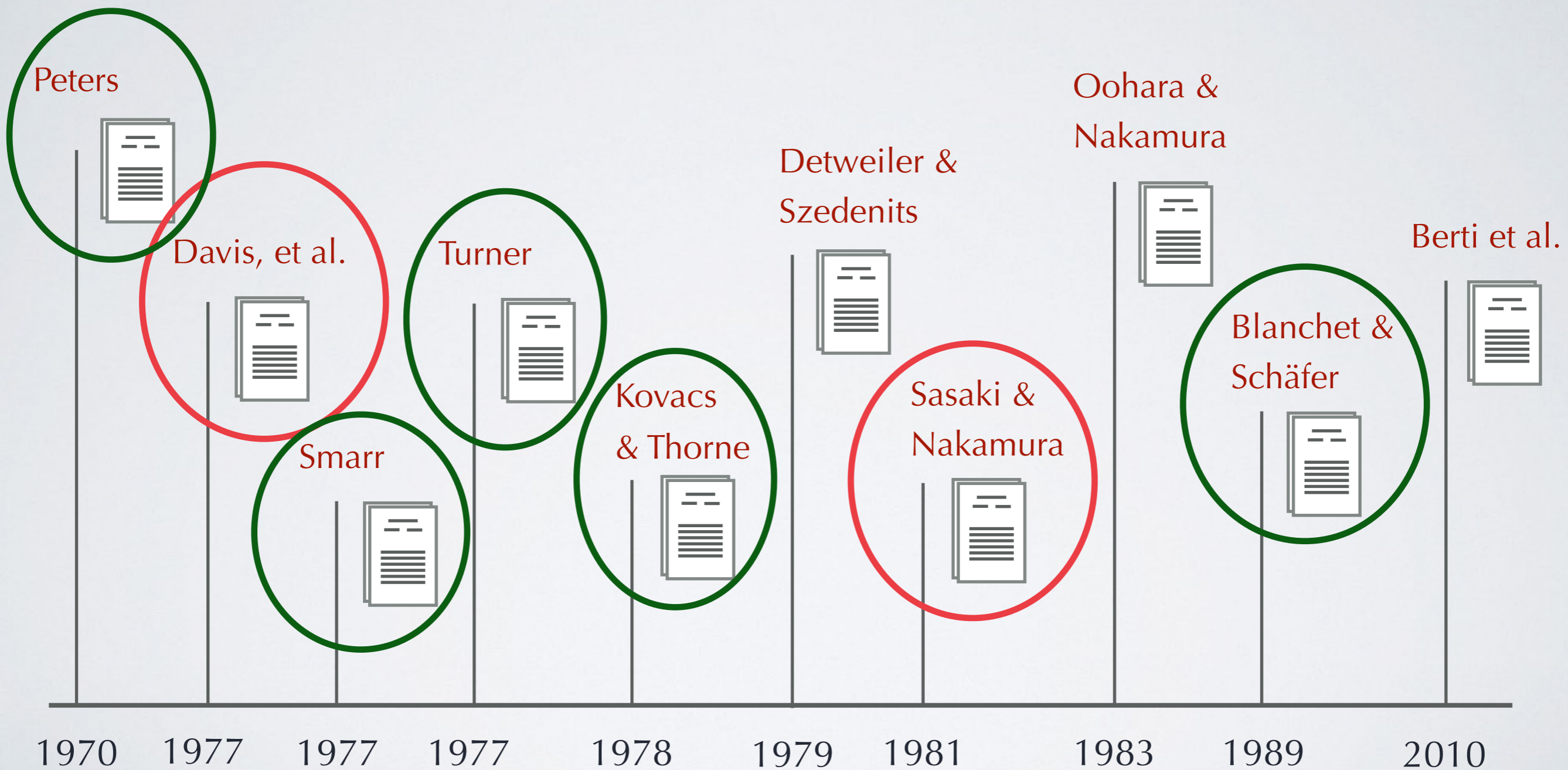
Local calculations



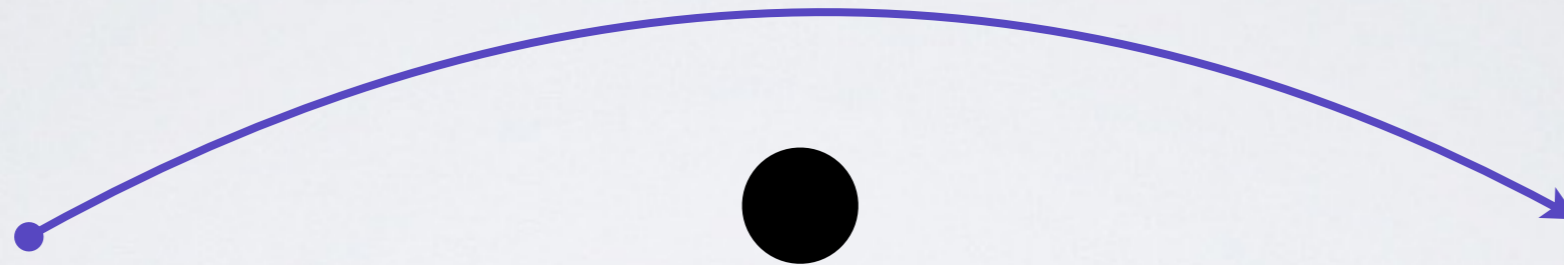
Wormholes and echoes



There has been a lot of previous work, but here are a couple highlights



Turner did the 'Peters-Mathews calculation' for scattering



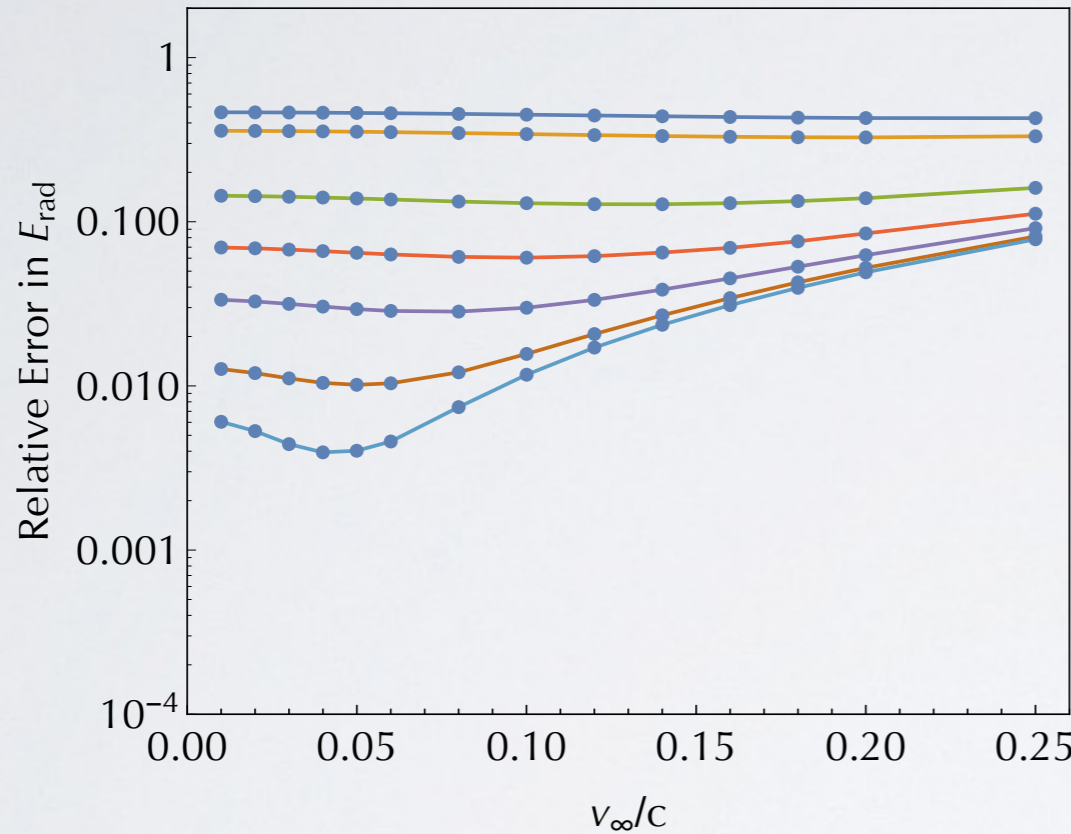
$$E_{\text{rad}} = \frac{8}{15} \frac{M^6 \mu^2}{J^7} \left[24 \arccos(-1/e) \left(1 + \frac{73}{24} e^2 + \frac{37}{96} e^4 \right) + (e^2 - 1)^{1/2} \left(\frac{301}{6} + \frac{673}{12} e^2 \right) \right], \quad e \geq 1$$

The Turner result has only been extended to 1PN



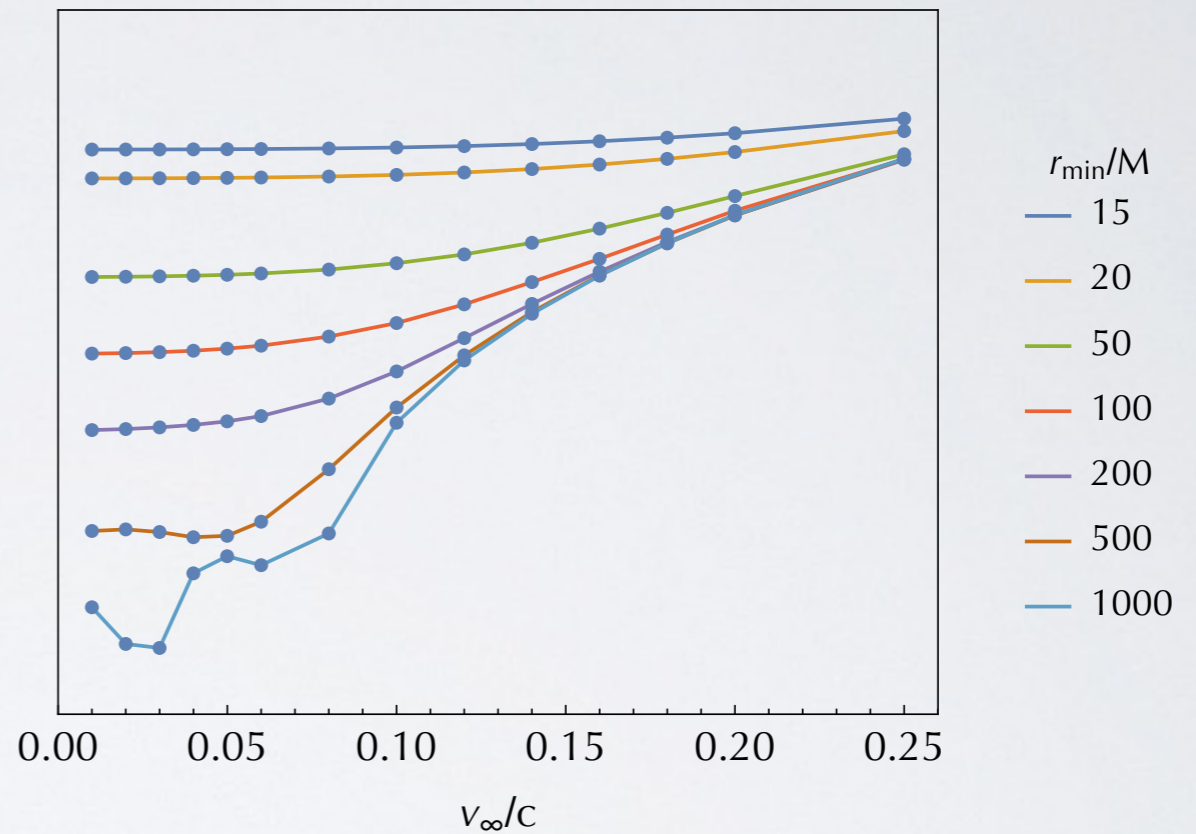
0PN

Error in Turner



1PN

Error in Blanchet & Schäfer



$$\cancel{v^2 \propto \frac{M}{r}}$$

We still use spectral methods in the unbound case



$$\left[-\frac{\partial^2}{\partial t^2} + \frac{\partial^2}{\partial r_*^2} - V_\ell(r) \right] \Psi_{\ell m}(t, r) = S_{\ell m}(t, r)$$

Bound



$$\Psi_{\ell m}(t, r) = \sum_{n=-\infty}^{\infty} X_{\ell mn}(r) e^{-i\omega_{mn}t}$$

$$S_{\ell m}(t, r) = \sum_{n=-\infty}^{\infty} Z_{\ell mn}(r) e^{-i\omega_{mn}t}$$



Unbound



$$\Psi_{\ell m}(t, r) = \frac{1}{2\pi} \int_{-\infty}^{\infty} X_{\ell m\omega}(r) e^{-i\omega t} d\omega$$

$$S_{\ell m}(t, r) = \frac{1}{2\pi} \int_{-\infty}^{\infty} Z_{\ell m\omega}(r) e^{-i\omega t} d\omega$$

$$\left[\frac{d^2}{dr_*^2} + \omega_{mn}^2 - V_\ell(r) \right] X_{\ell mn}(r) = Z_{\ell mn}(r)$$



$$\left[\frac{d^2}{dr_*^2} + \omega^2 - V_\ell(r) \right] X_{\ell m\omega}(r) = Z_{\ell m\omega}(r).$$

The particular solution follows from integrating
over the source



Time domain

$$\left[-\frac{\partial^2}{\partial t^2} + \frac{\partial^2}{\partial r_*^2} - V_\ell(r) \right] \Psi_{\ell m}(t, r) = \underline{G_{\ell m}(t)} \delta[r - r_p(t)] + \underline{F_{\ell m}(t)} \delta'[r - r_p(t)]$$

Frequency domain

$$\left[\frac{d^2}{dr_*^2} + \omega^2 - V_\ell(r) \right] X_{\ell m \omega}(r) = Z_{\ell m \omega}(r).$$

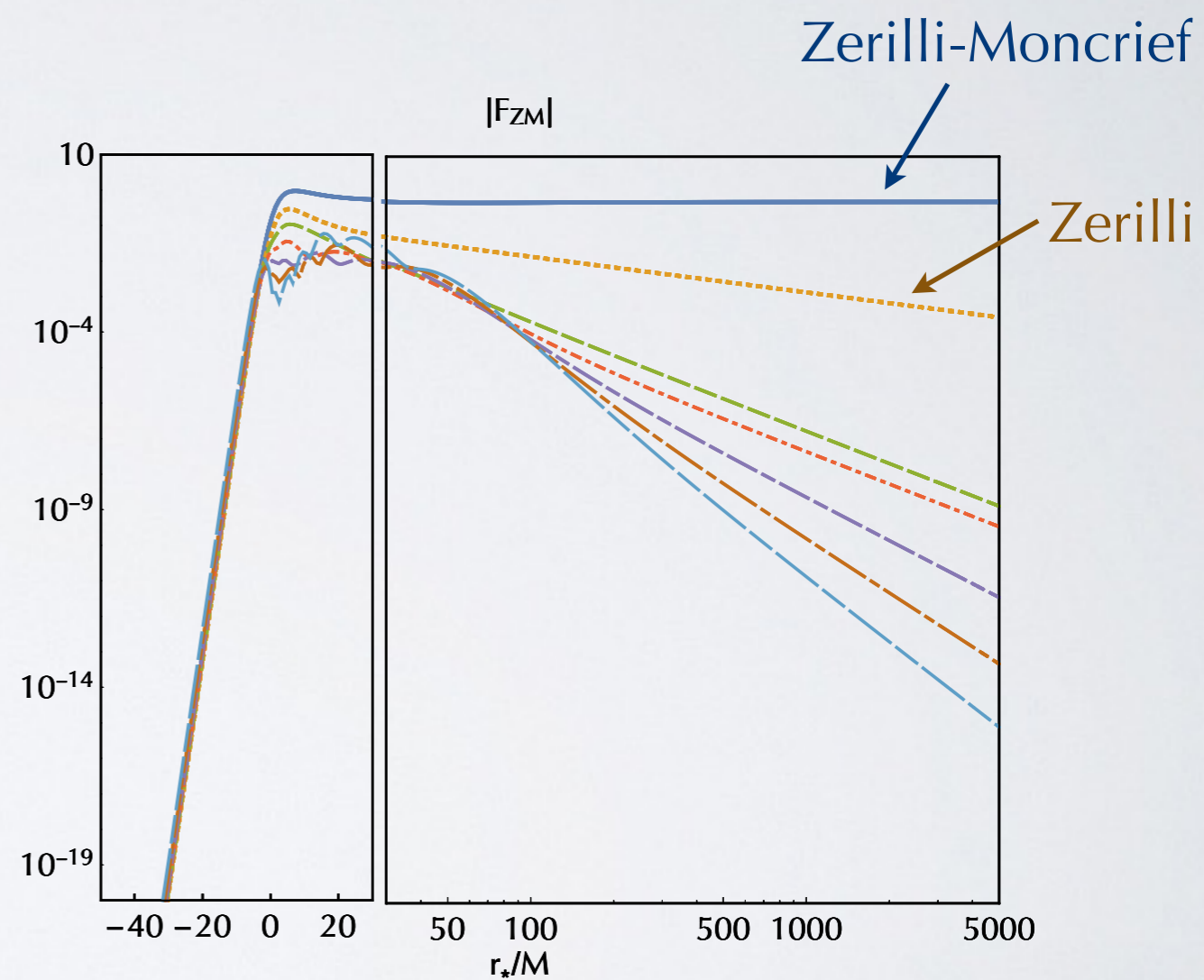
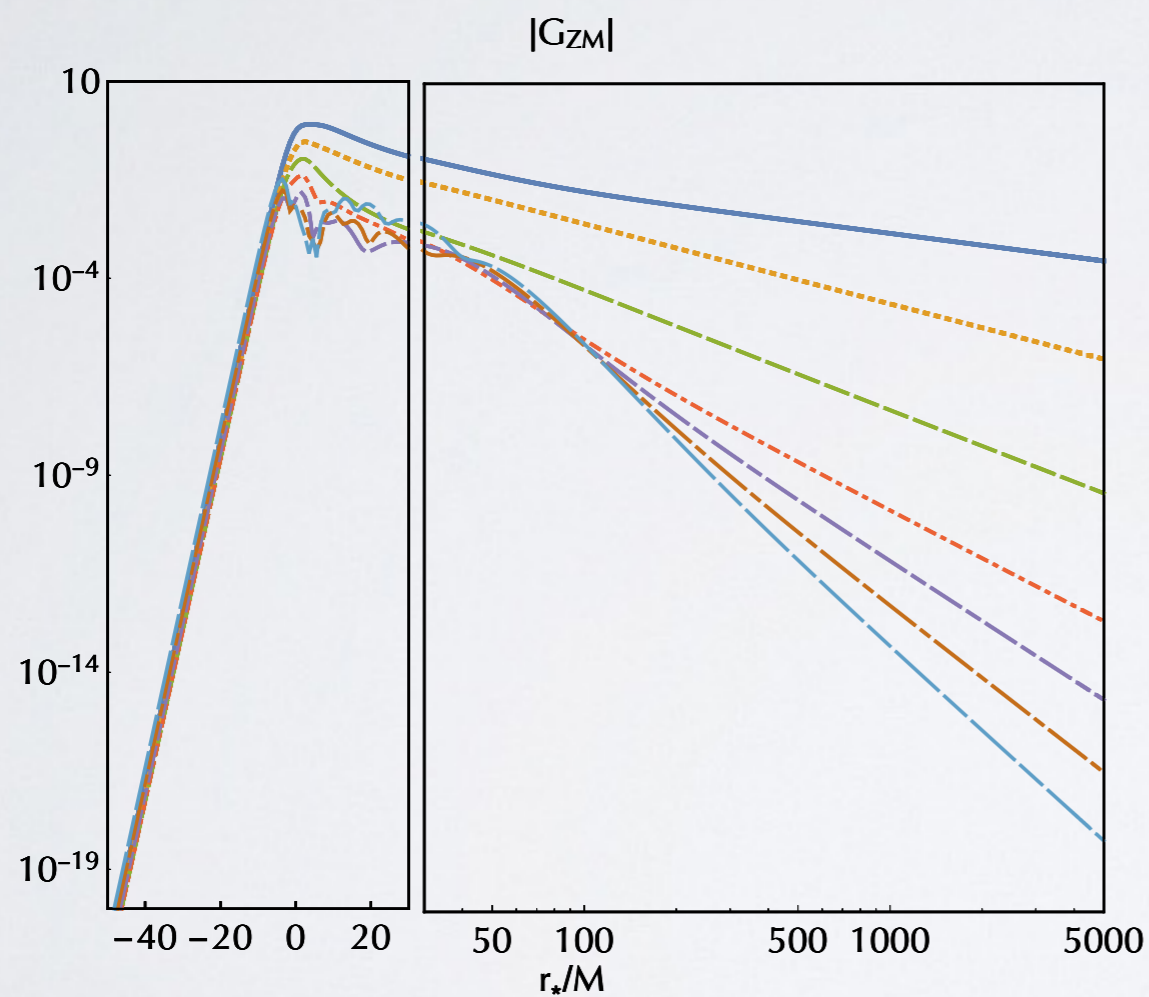
$$C_{\ell m \omega}^\pm \sim \int_{-\infty}^{\infty} dt \left(\hat{X}_{\ell m \omega}^\mp \underline{G_{\ell m}} + \frac{d\hat{X}_{\ell m \omega}^\mp}{dr} \underline{F_{\ell m}} \right)$$

$$\Psi_{\ell m}^\pm(t, r) \equiv \frac{1}{2\pi} \int_{-\infty}^{\infty} C_{\ell m \omega}^\pm \hat{X}_{\ell m \omega}^\pm(r) e^{-i\omega t} d\omega$$

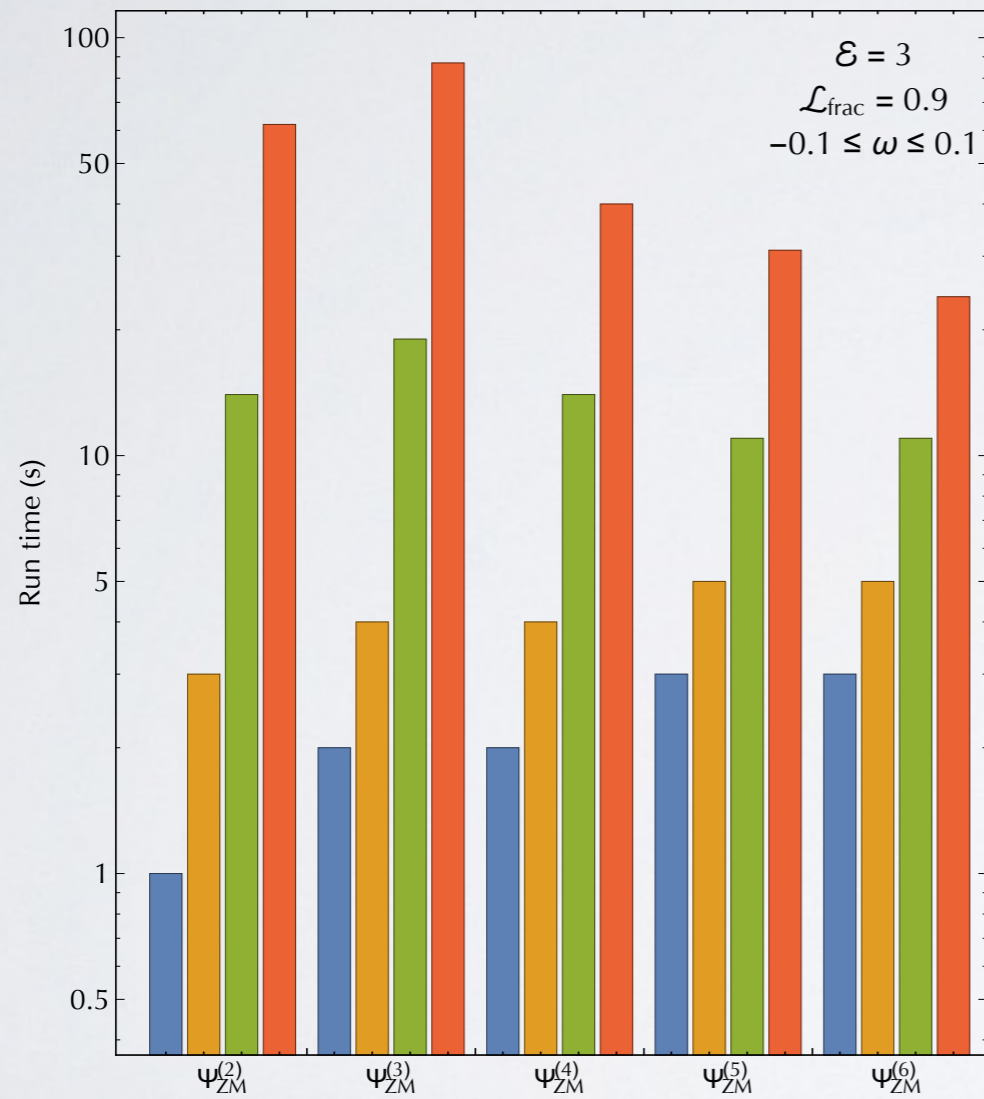
Convergence depends on which master function you choose



$$C_{lm\omega}^{\pm} \sim \int_{-\infty}^{\infty} dt \left(\hat{X}_{lm\omega}^{\mp} G_{lm} + \frac{d\hat{X}_{lm\omega}^{\mp}}{dr} F_{lm} \right)$$

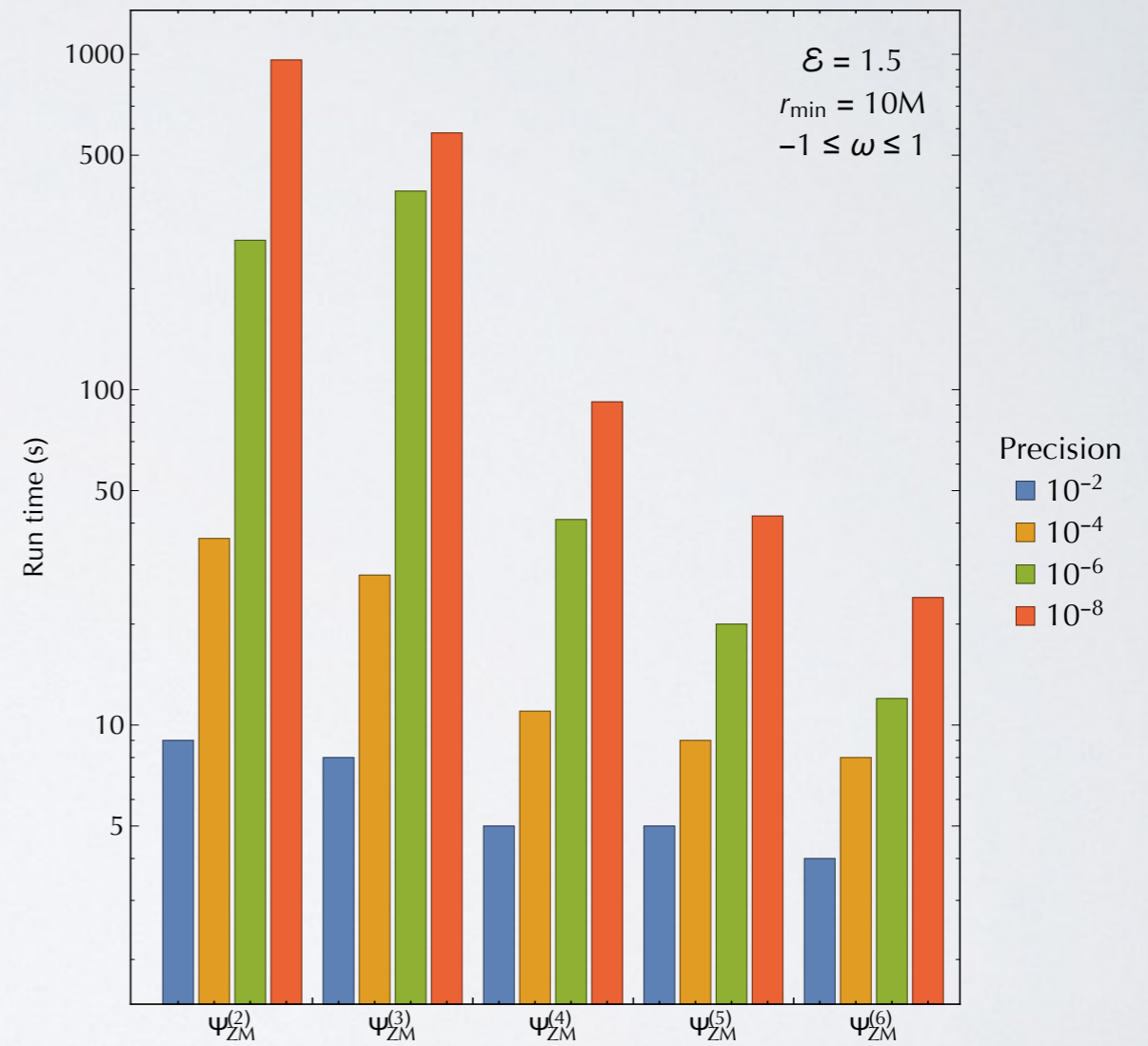


Speed benefits come at large frequencies



Precision

- 10^{-2}
- 10^{-4}
- 10^{-6}
- 10^{-8}



Precision

- 10^{-2}
- 10^{-4}
- 10^{-6}
- 10^{-8}

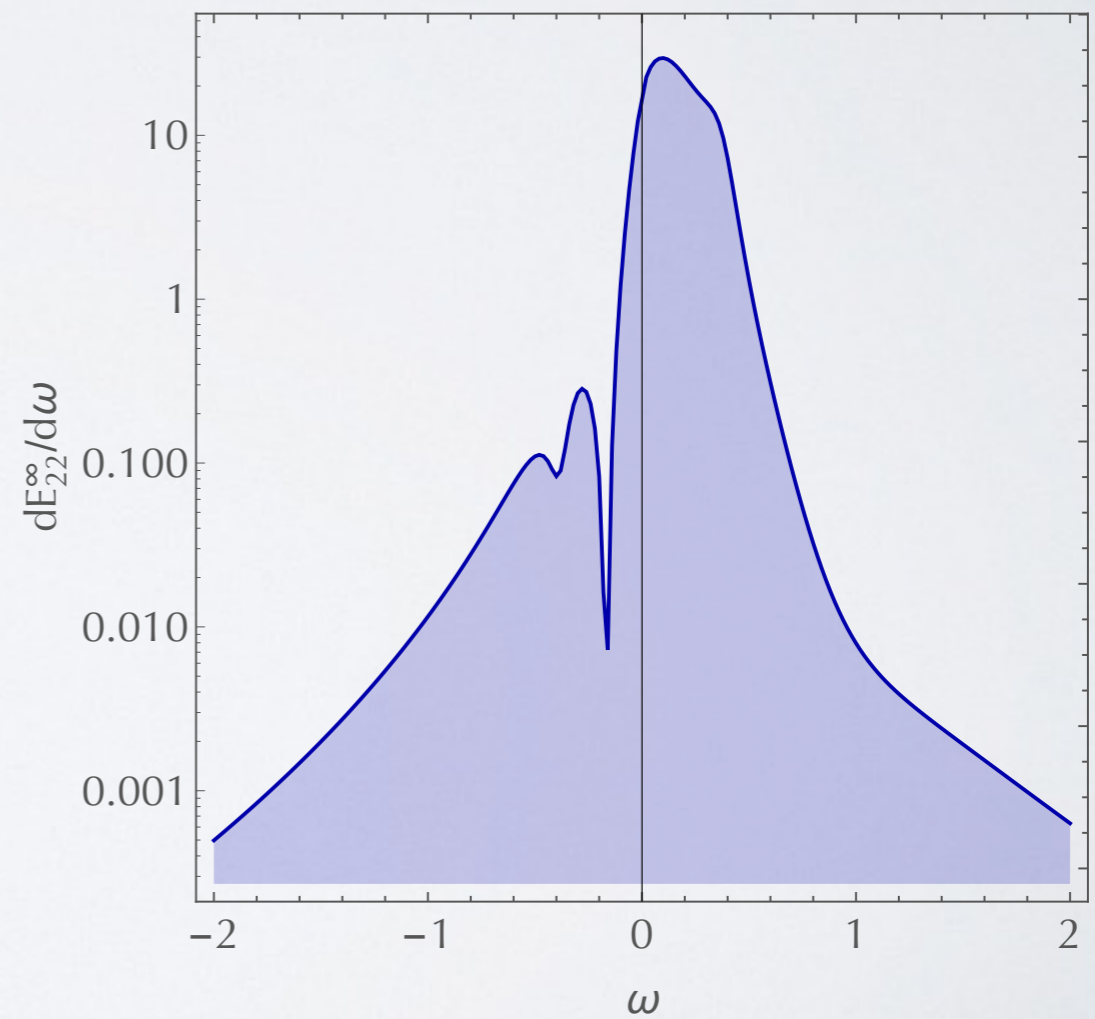
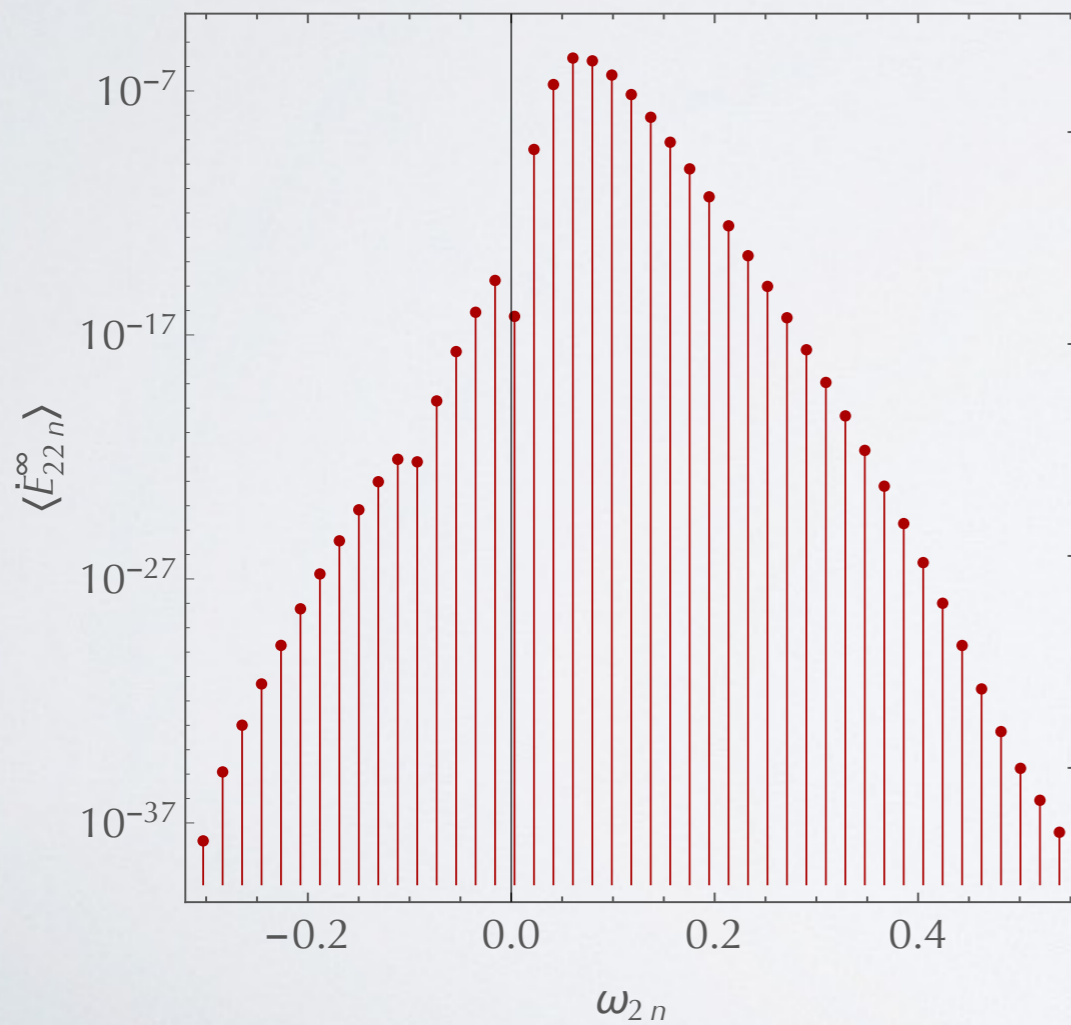
The unbound spectrum is dense



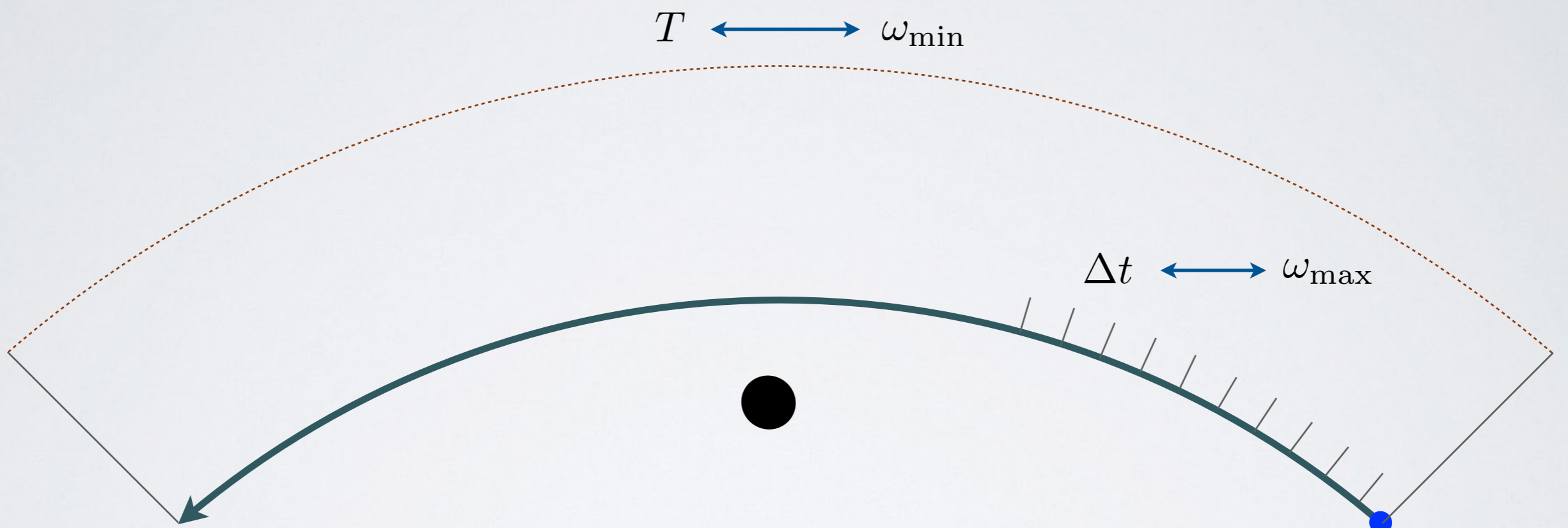
$(p, e) = (10, 0.2)$



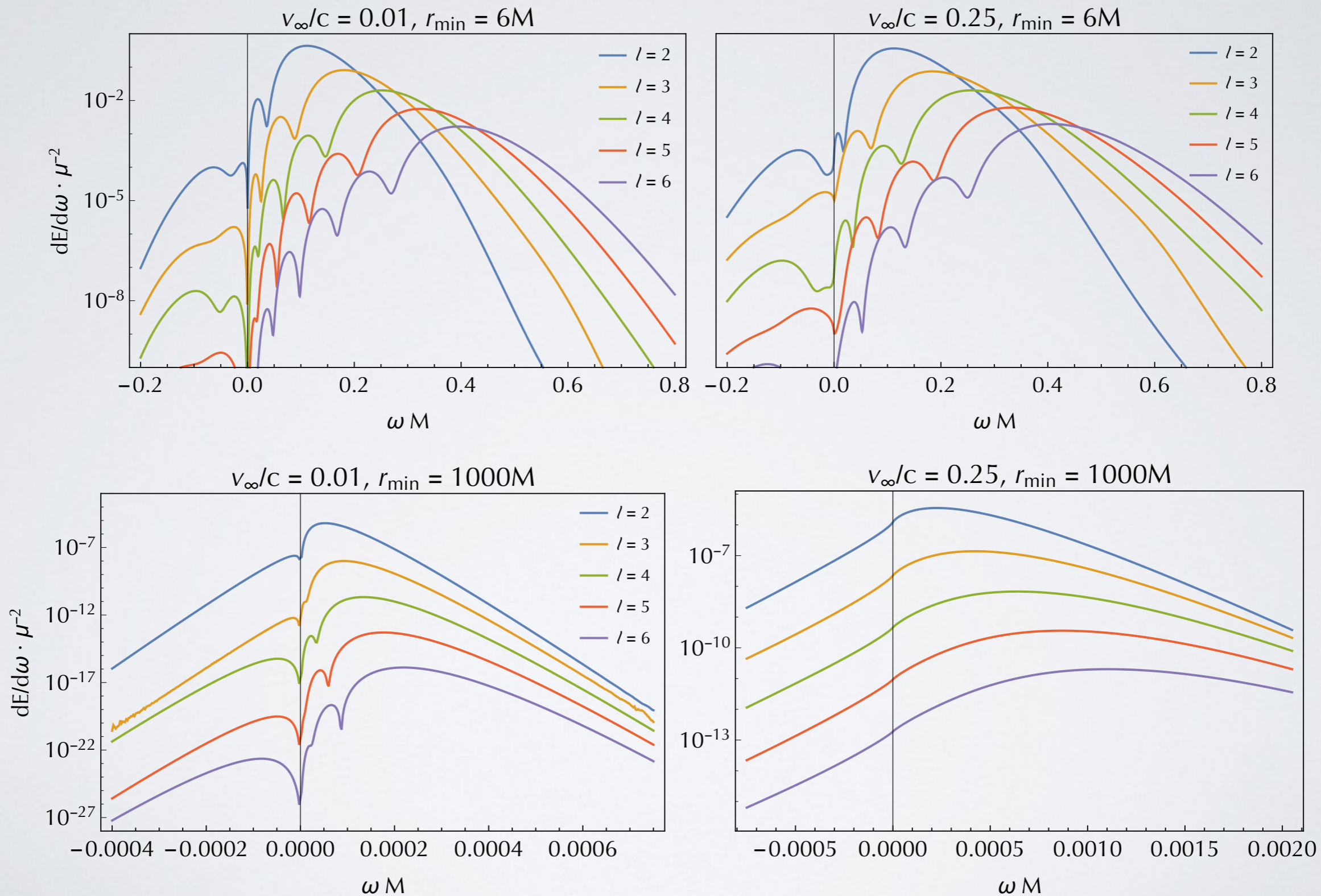
$(\mathcal{E}, r_{\min}) = (1.5, 4.3M)$



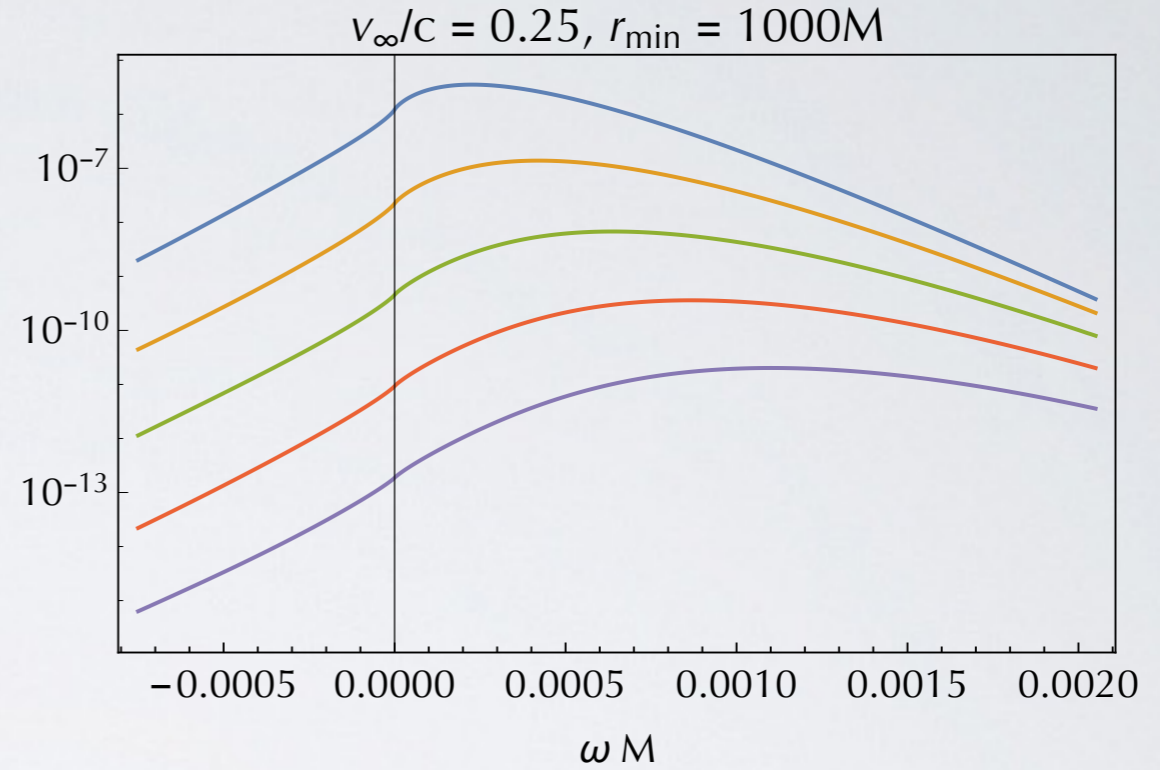
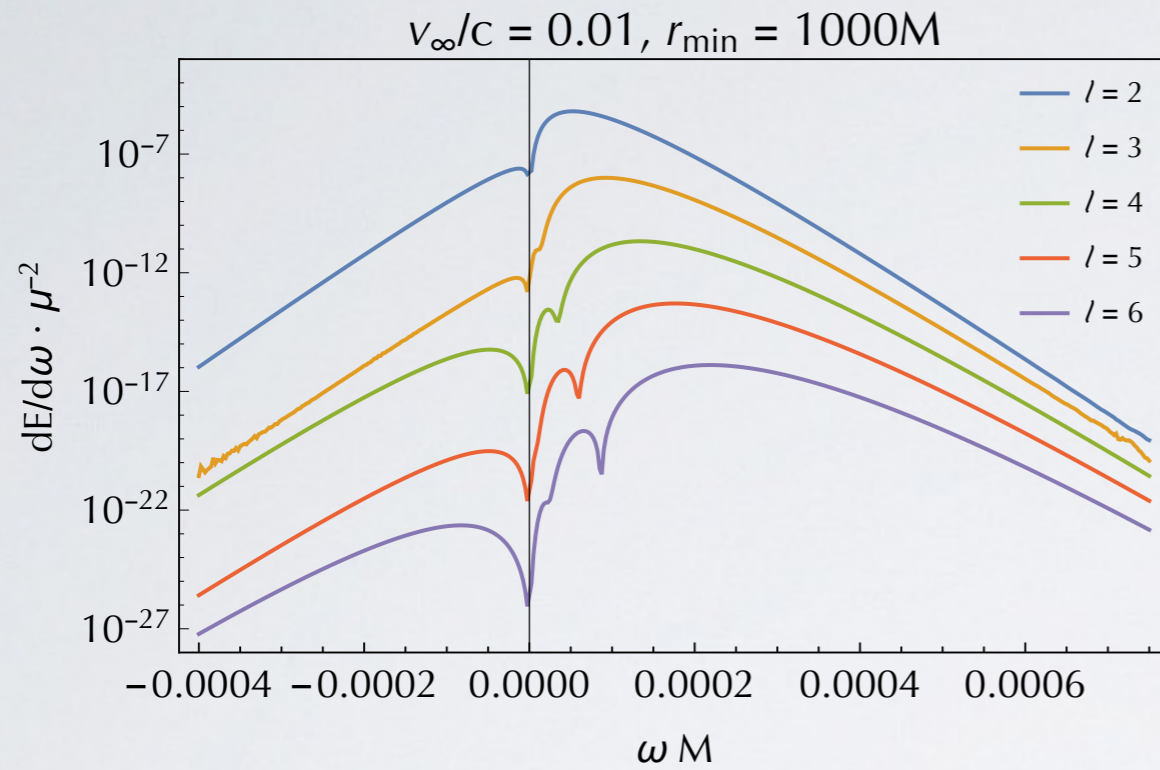
The time domain is dense, too



The character of spectra changes with r_{\min}

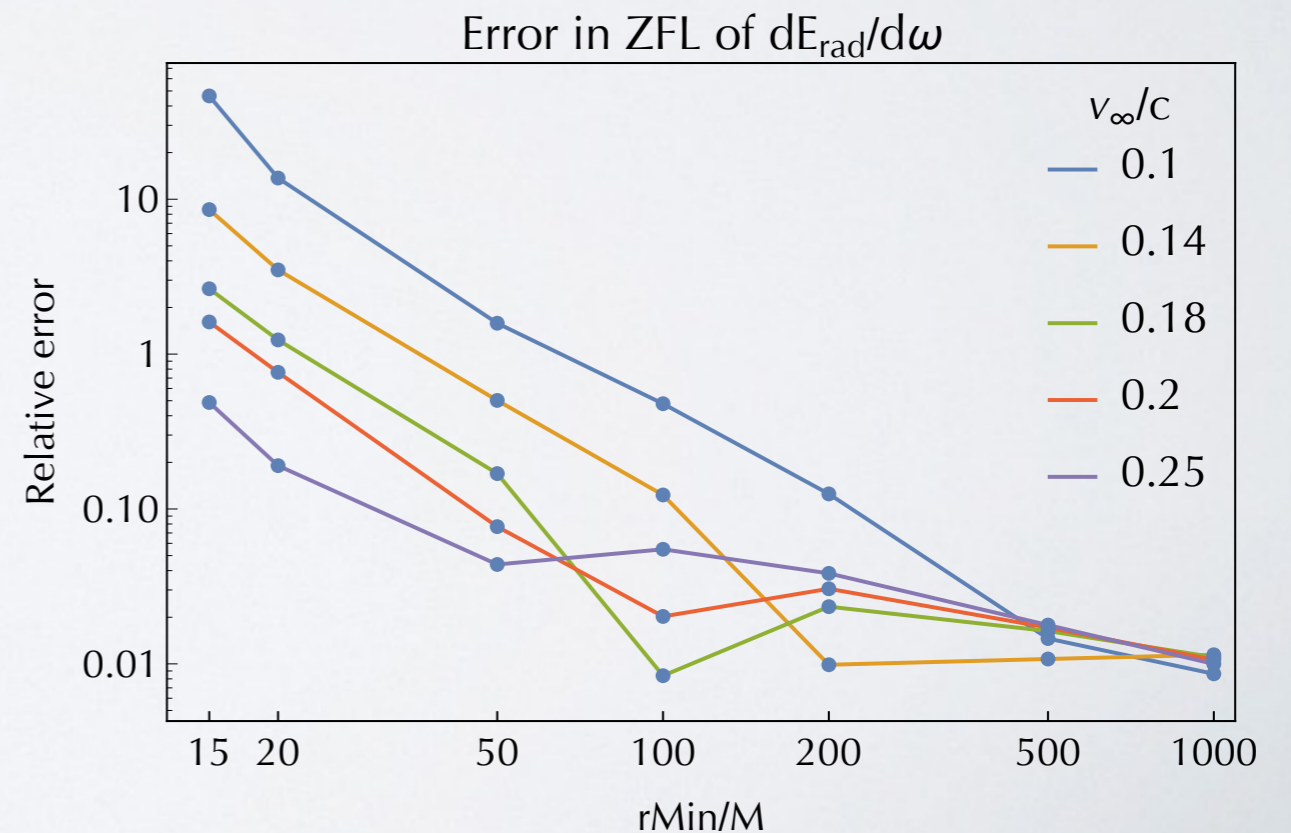


Smarr predicted the zero-frequency-limit to be non-zero for unbound motion

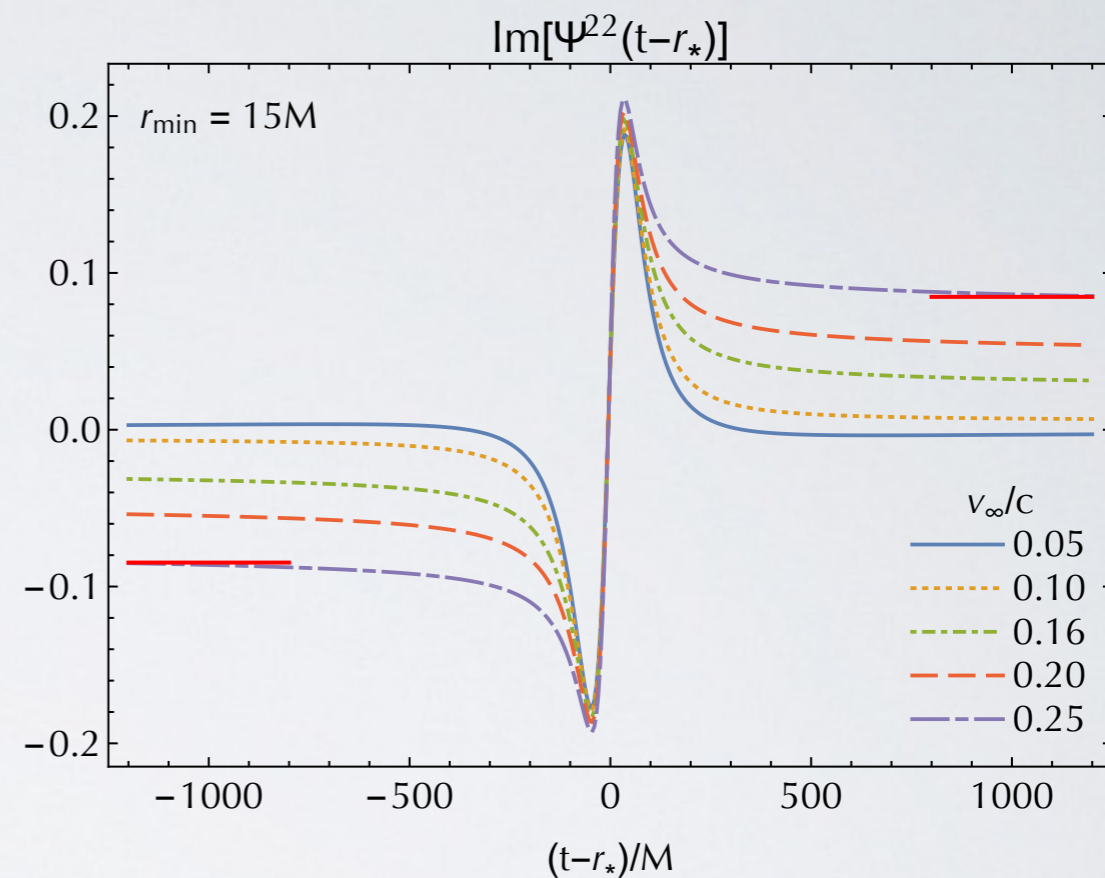
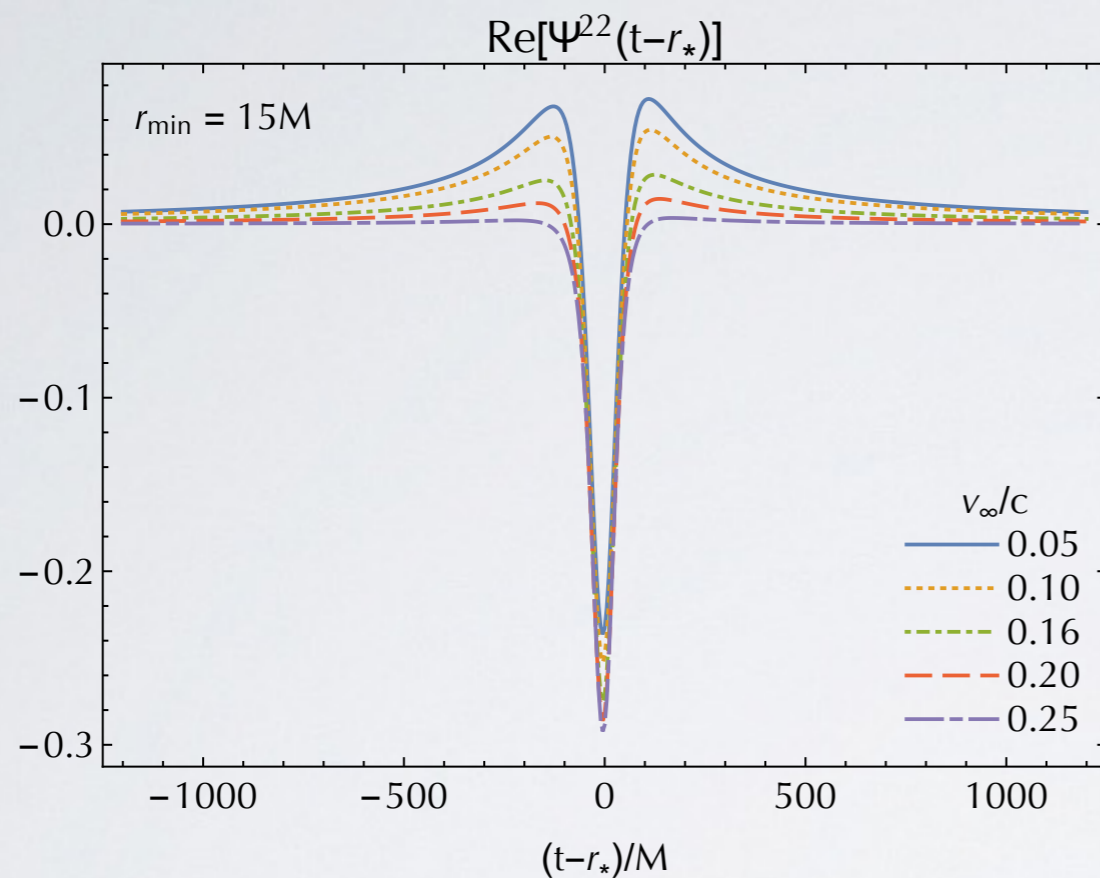


Smarr, 1977:

$$\left(\frac{dE}{d\omega}\right)_{\omega \rightarrow 0} = \frac{4}{\pi} \frac{\mu^2 M^2 \mathcal{E}^2 (1+v^2)^2}{b^2 v^4} \left[2 - \frac{16}{3} v^2 + \left(3v - \frac{1}{v} \right) \log \left(\frac{1+v}{1-v} \right) \right]$$



The ZFL also predicts the memory effect



$$\Psi_{lm}(u, r_* \rightarrow \infty) = \frac{1}{2\pi} \int_{-\infty}^{\infty} C_{lm\omega}^+ e^{-i\omega u} d\omega$$

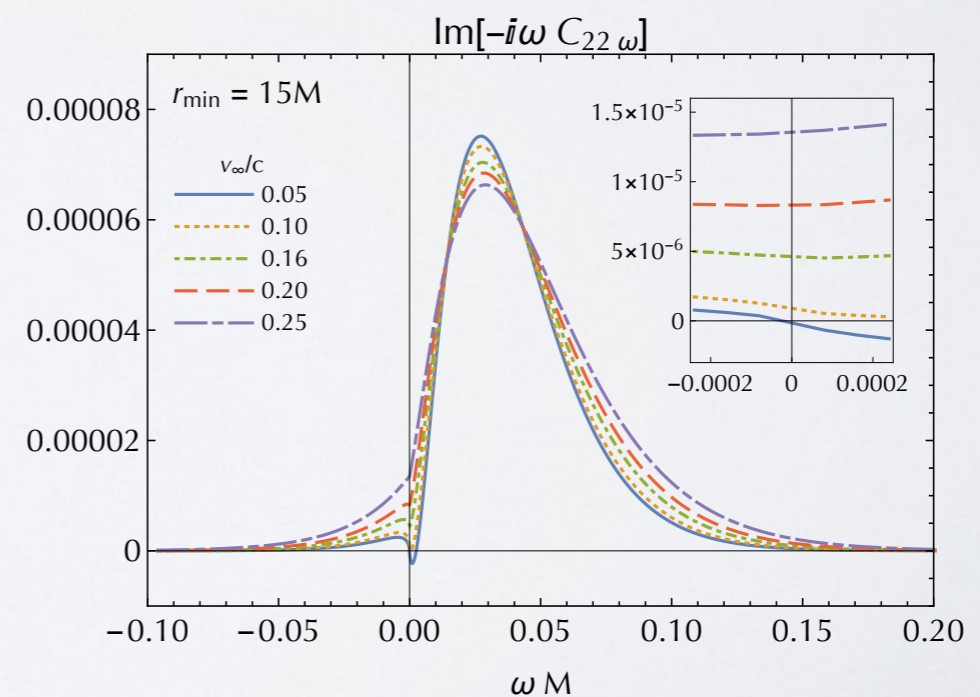
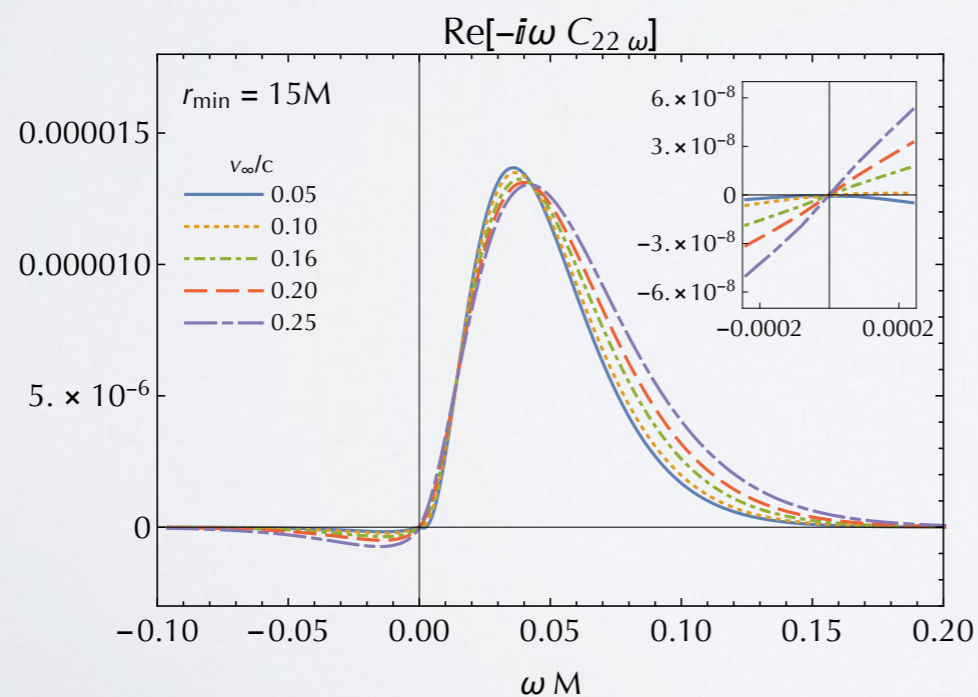
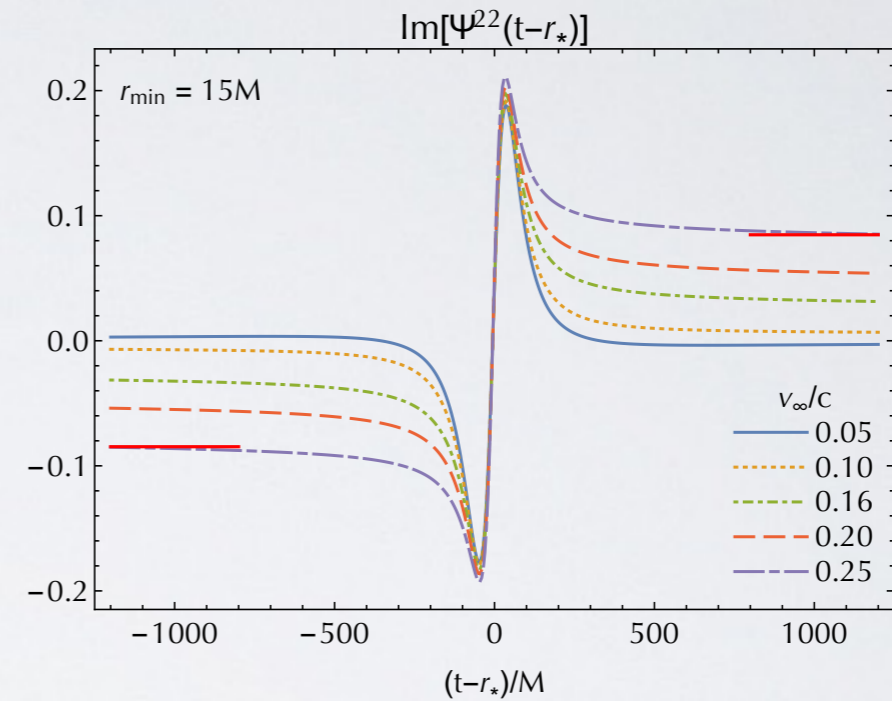
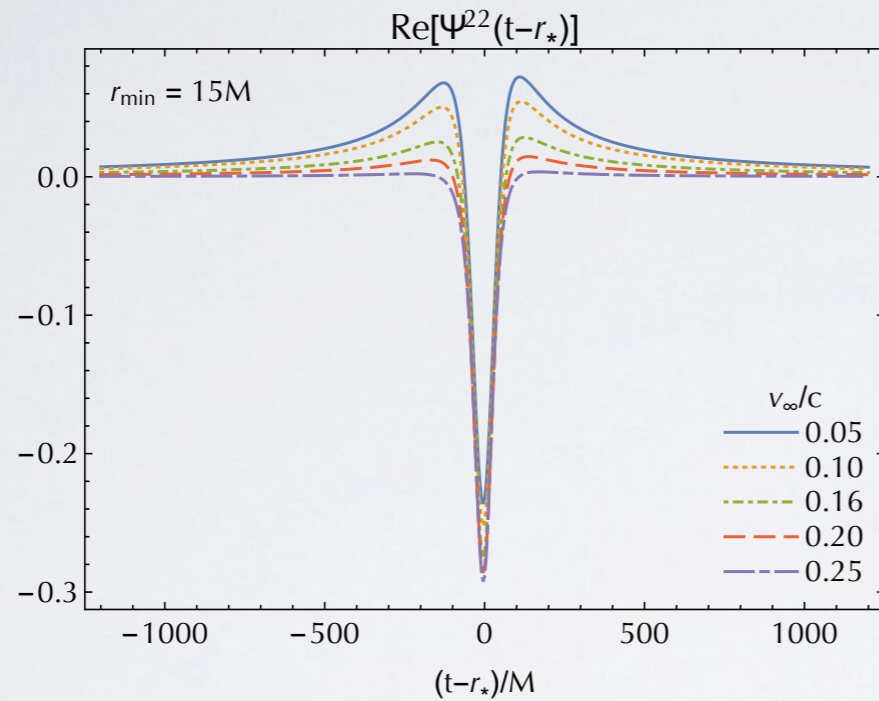
$$\Psi_{lm}(\infty, r_*) - \Psi_{lm}(-\infty, r_*) = \lim_{\omega \rightarrow 0} \int_{-\infty}^{\infty} e^{i\omega u} \partial_u \Psi_{lm}(u, r_*) du$$

$$\llbracket \Psi_{lm} \rrbracket = \lim_{\omega \rightarrow 0} \int_{-\infty}^{\infty} e^{i\omega u} \partial_u \left(\frac{1}{2\pi} \int_{-\infty}^{\infty} C_{lm\omega'}^+ e^{-i\omega' u} d\omega' \right) du = - \lim_{\omega \rightarrow 0} i\omega C_{lm\omega}^+$$

The ZFL also predicts the memory effect



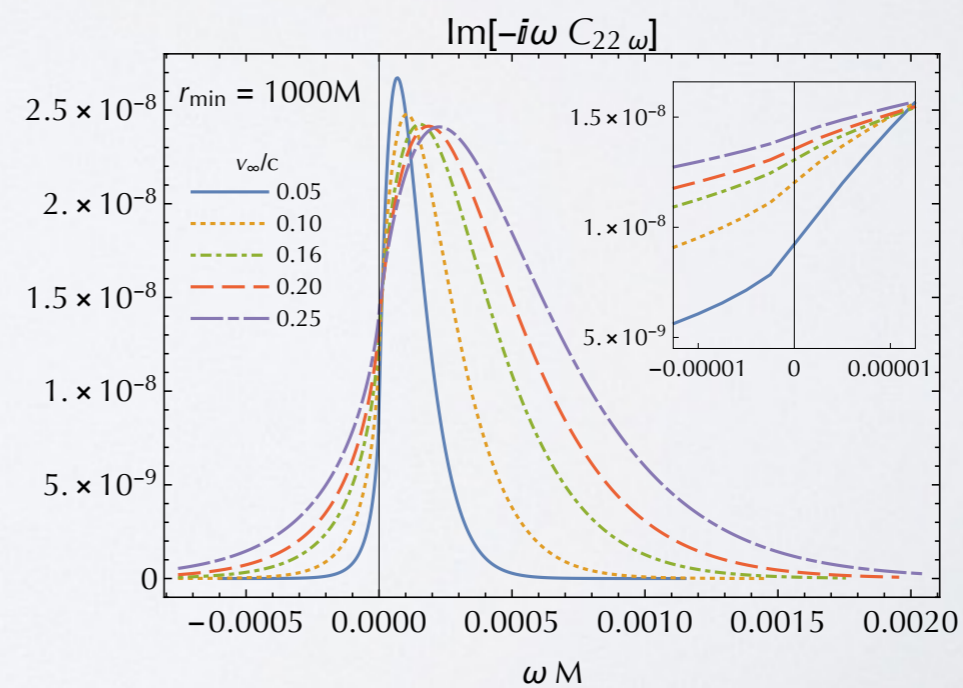
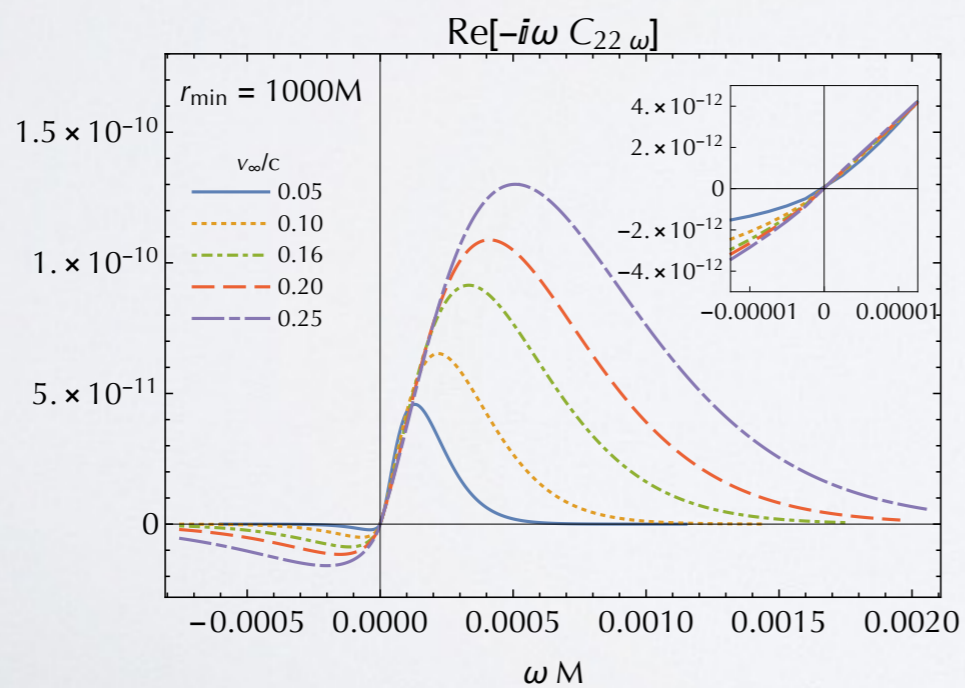
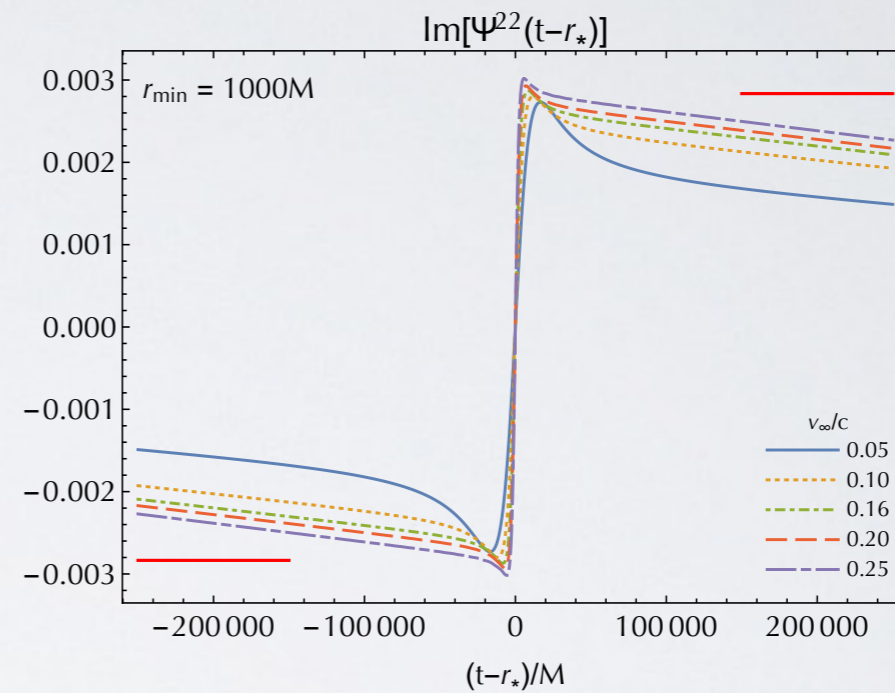
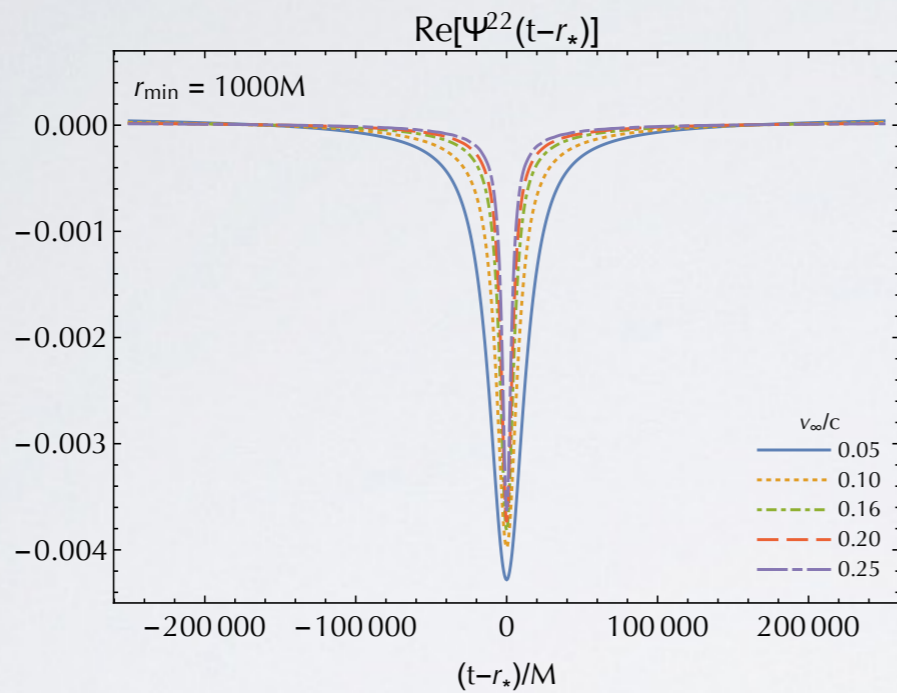
$$[\Psi_{lm}] = - \lim_{\omega \rightarrow 0} i\omega C_{lm\omega}^+$$



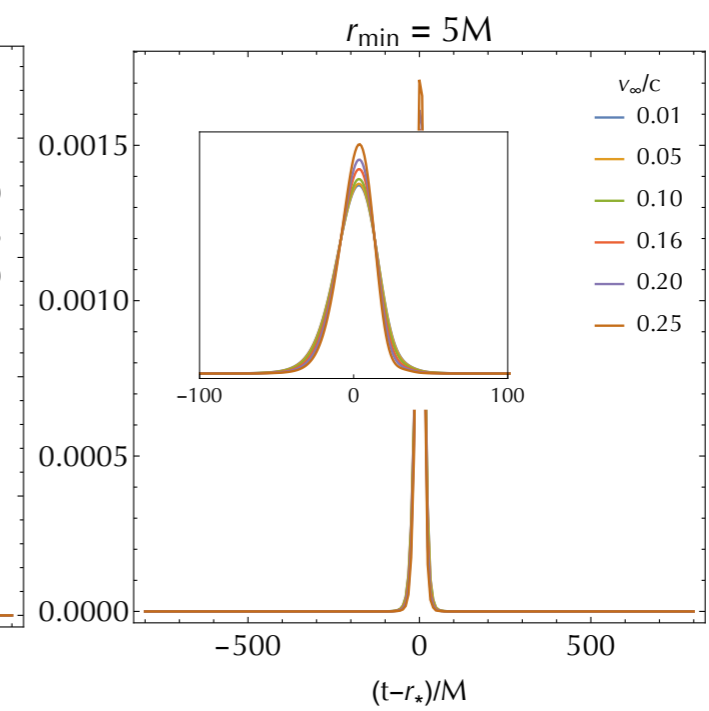
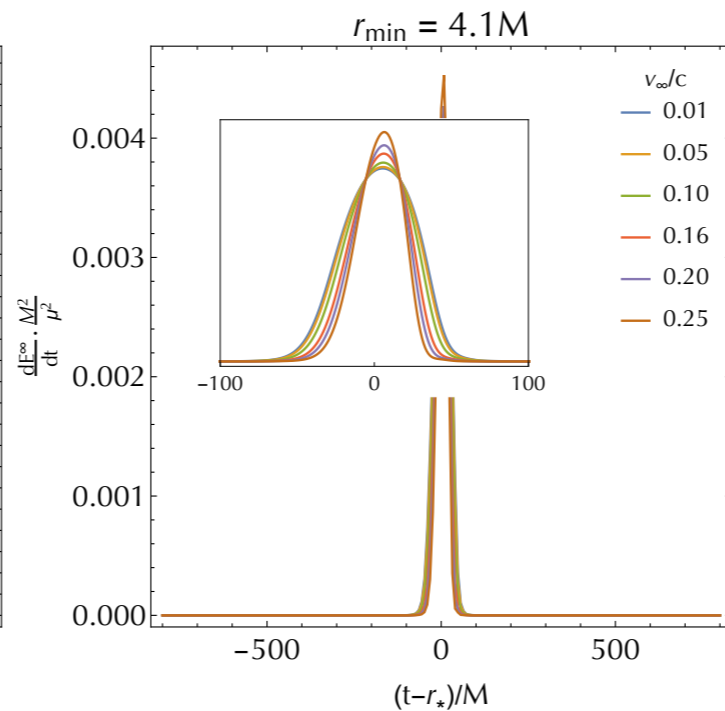
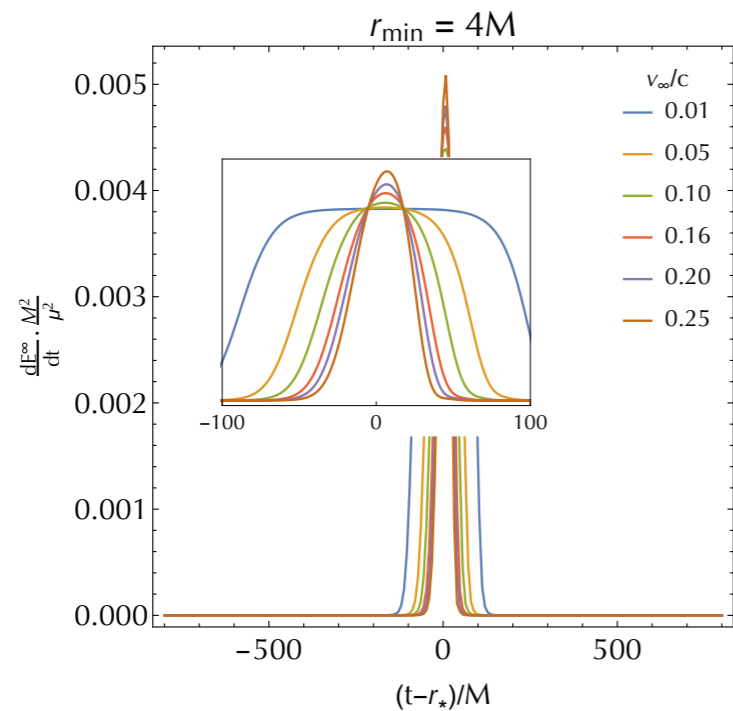
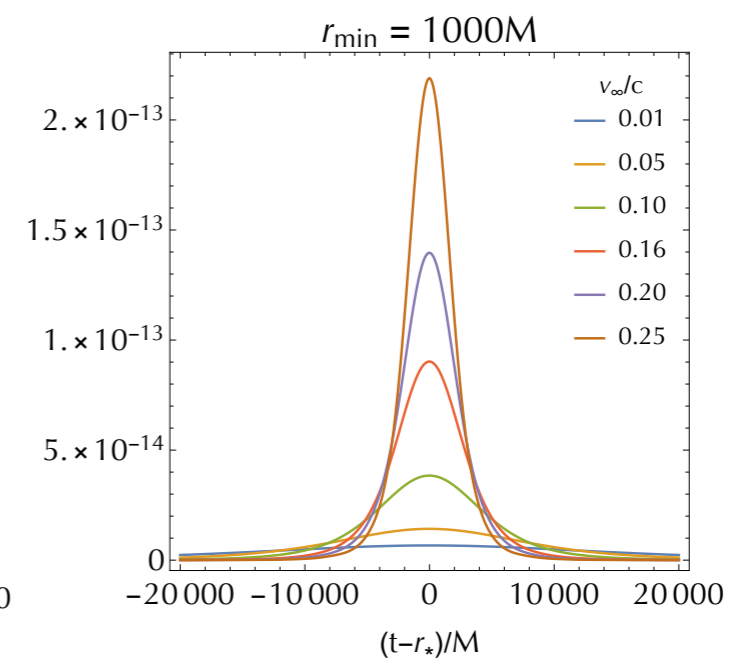
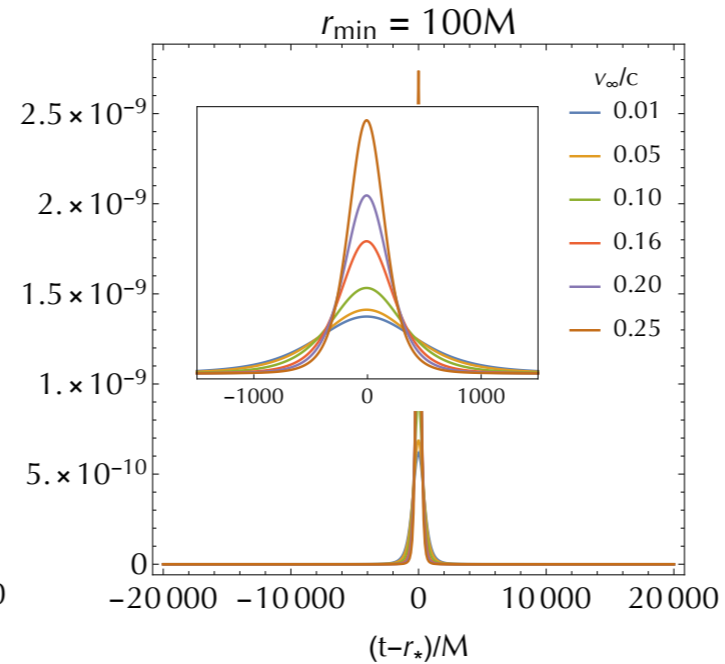
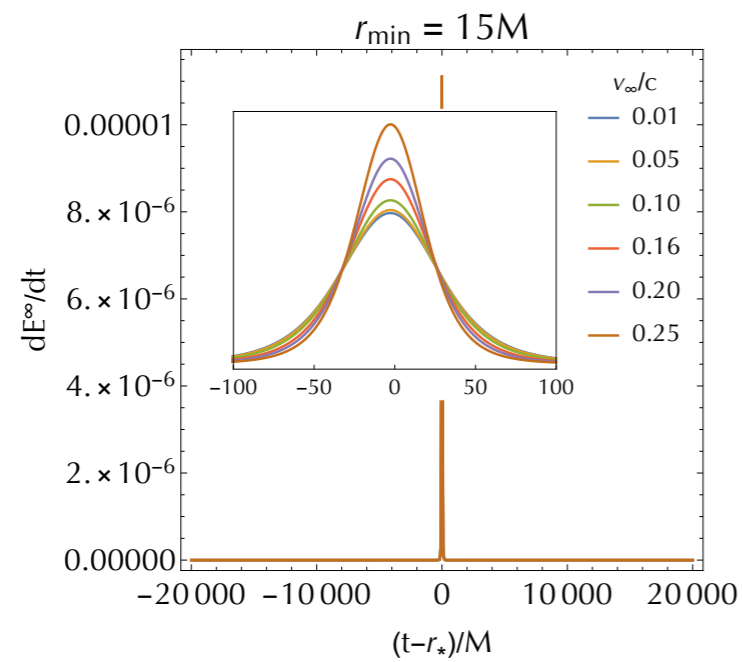
The code struggles with small frequencies



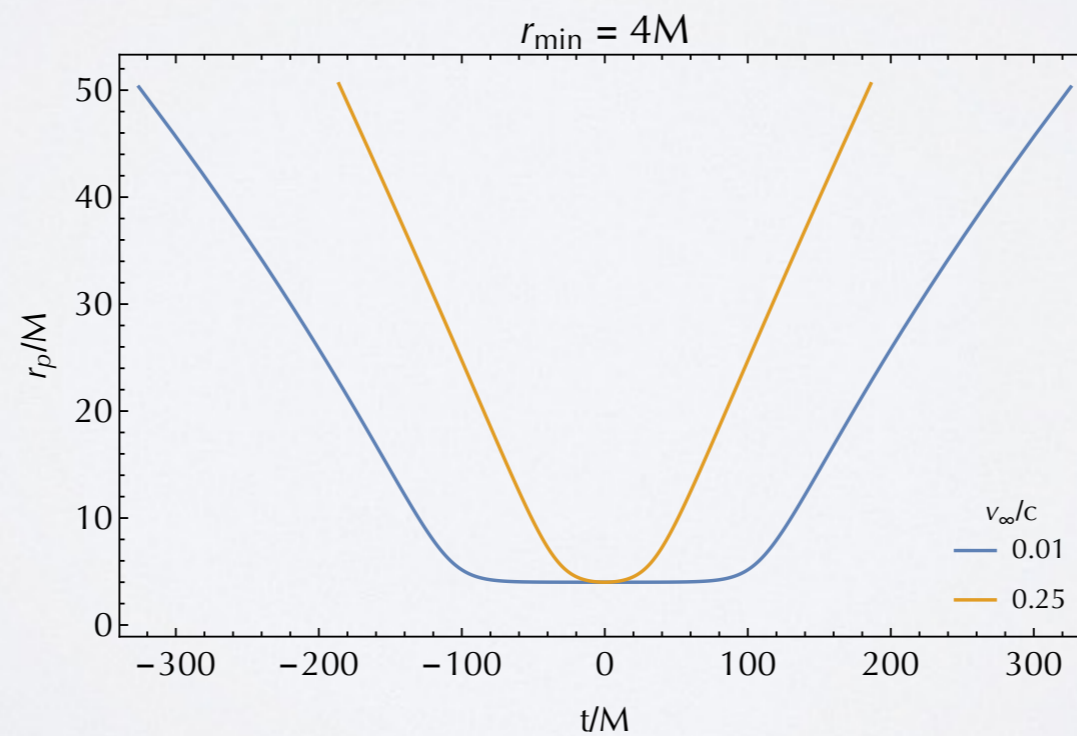
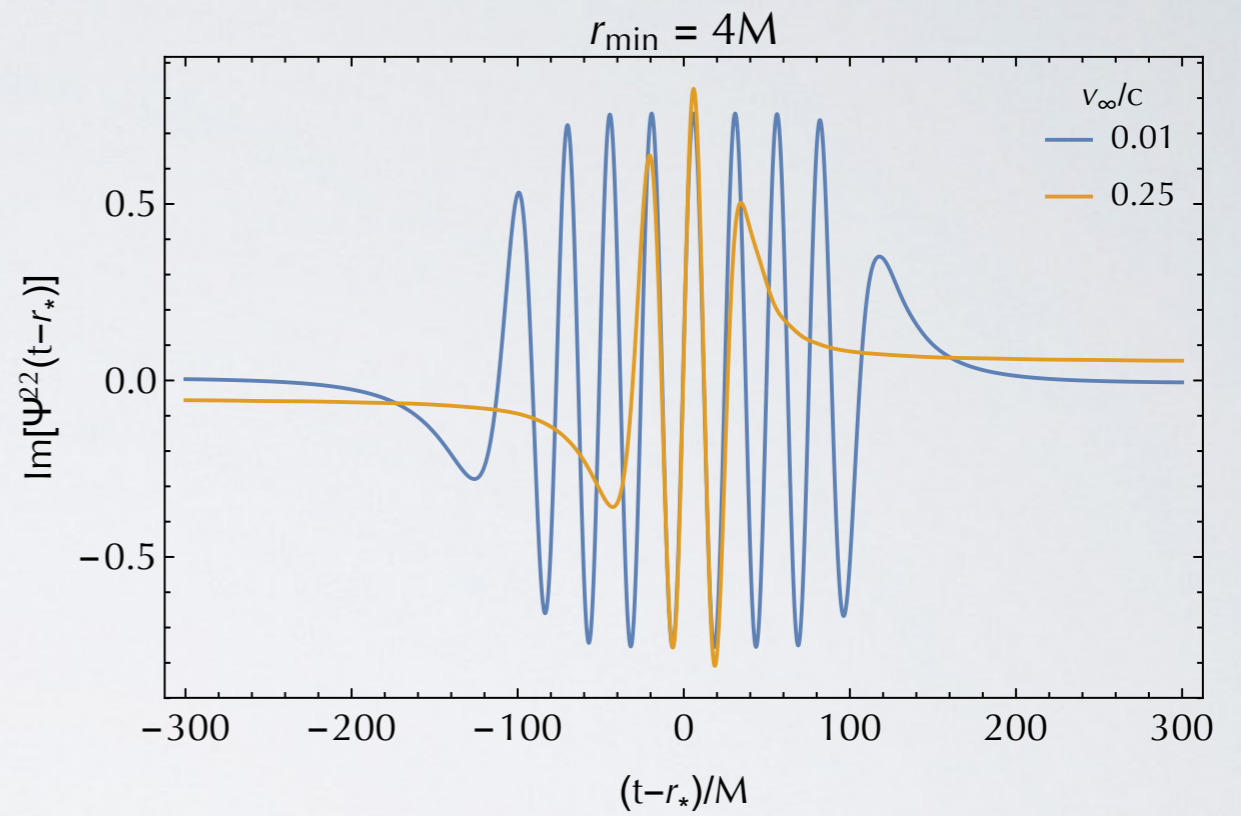
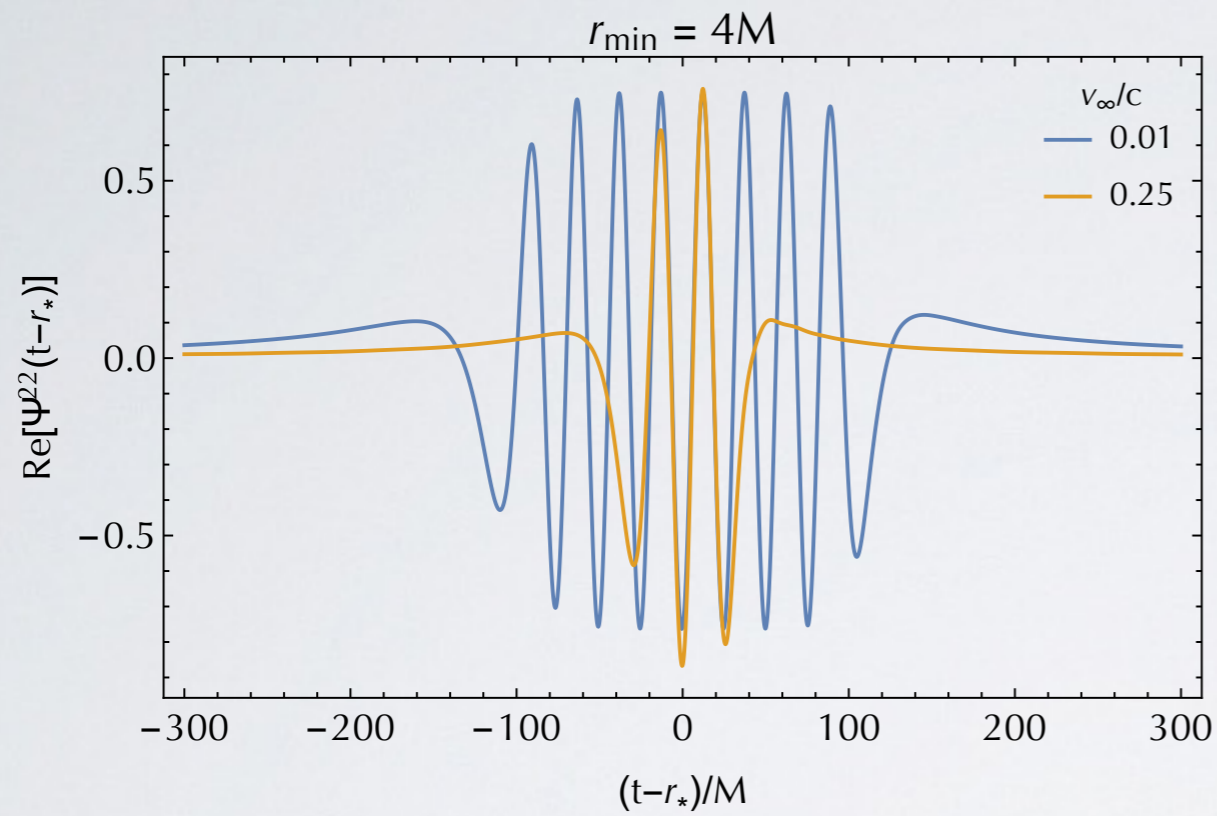
$$[\Psi_{lm}] = - \lim_{\omega \rightarrow 0} i\omega C_{lm\omega}^+$$



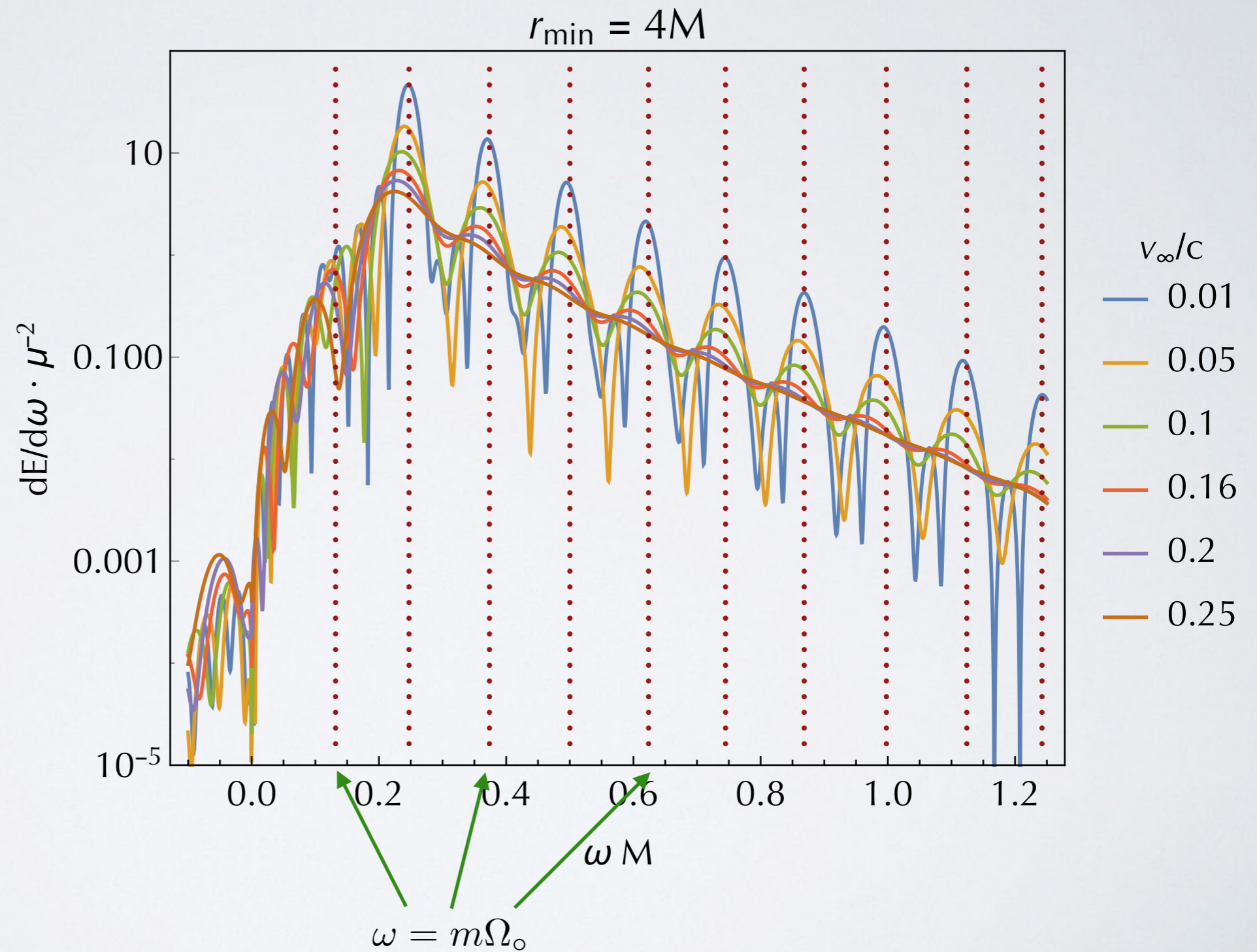
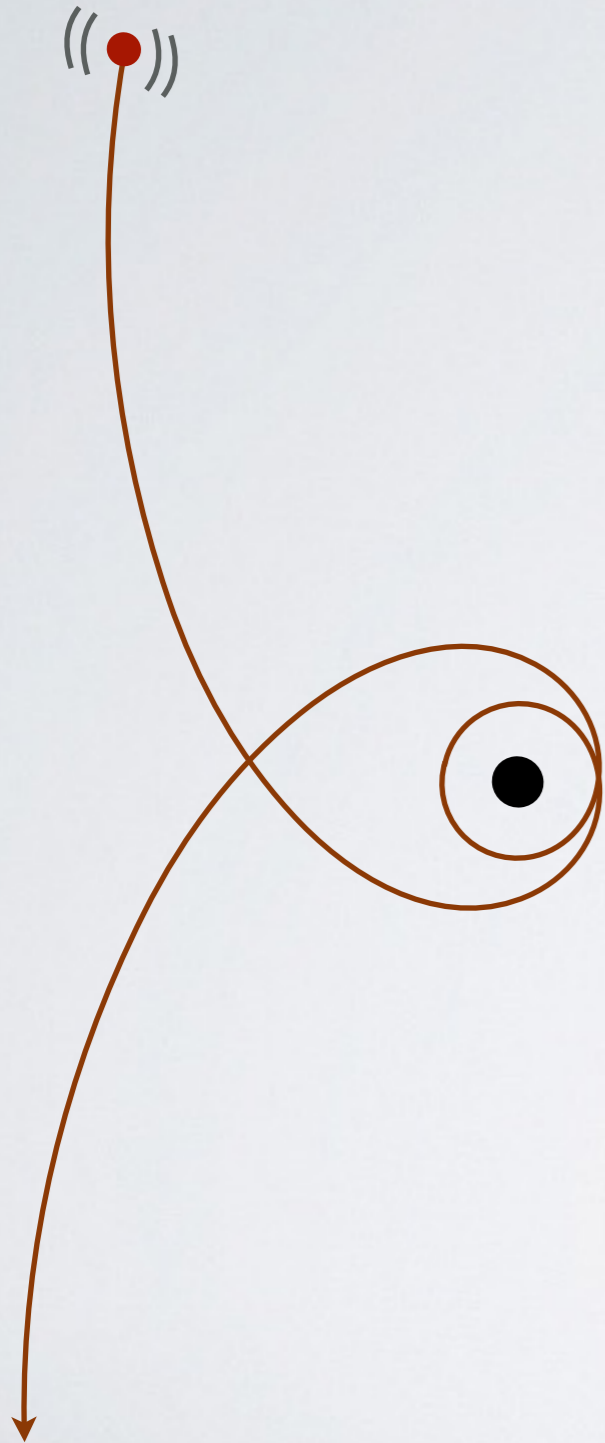
The energy flux is interesting in the large and small limits



At the critical surface the particle will radiate forever



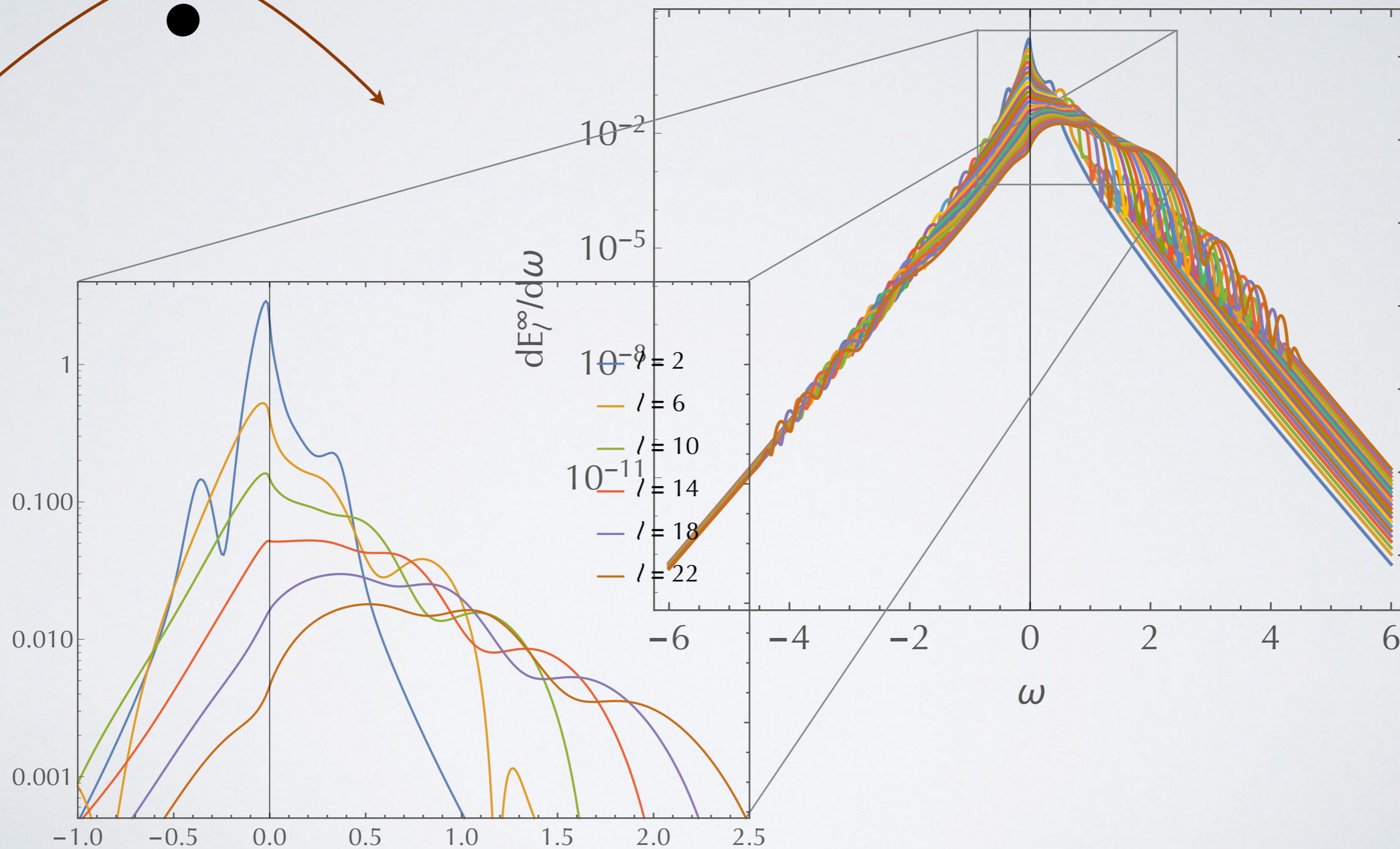
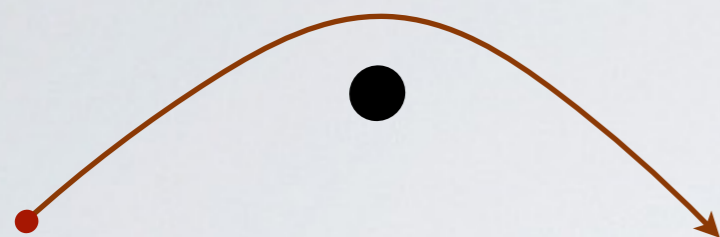
At the critical surface the harmonics are evident



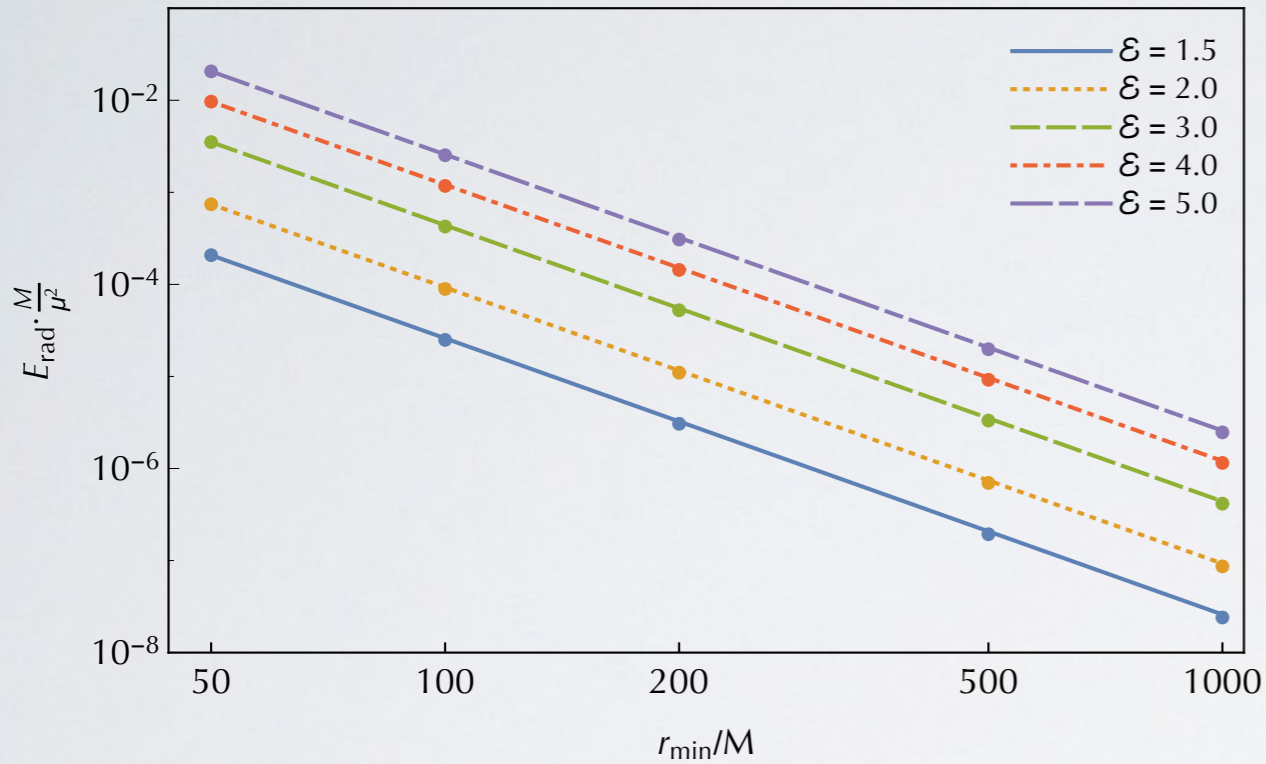
Frequency domain allows high Lorentz factor scatters



$(\mathcal{E}, b) = (10, 20M), v/c = 0.995$

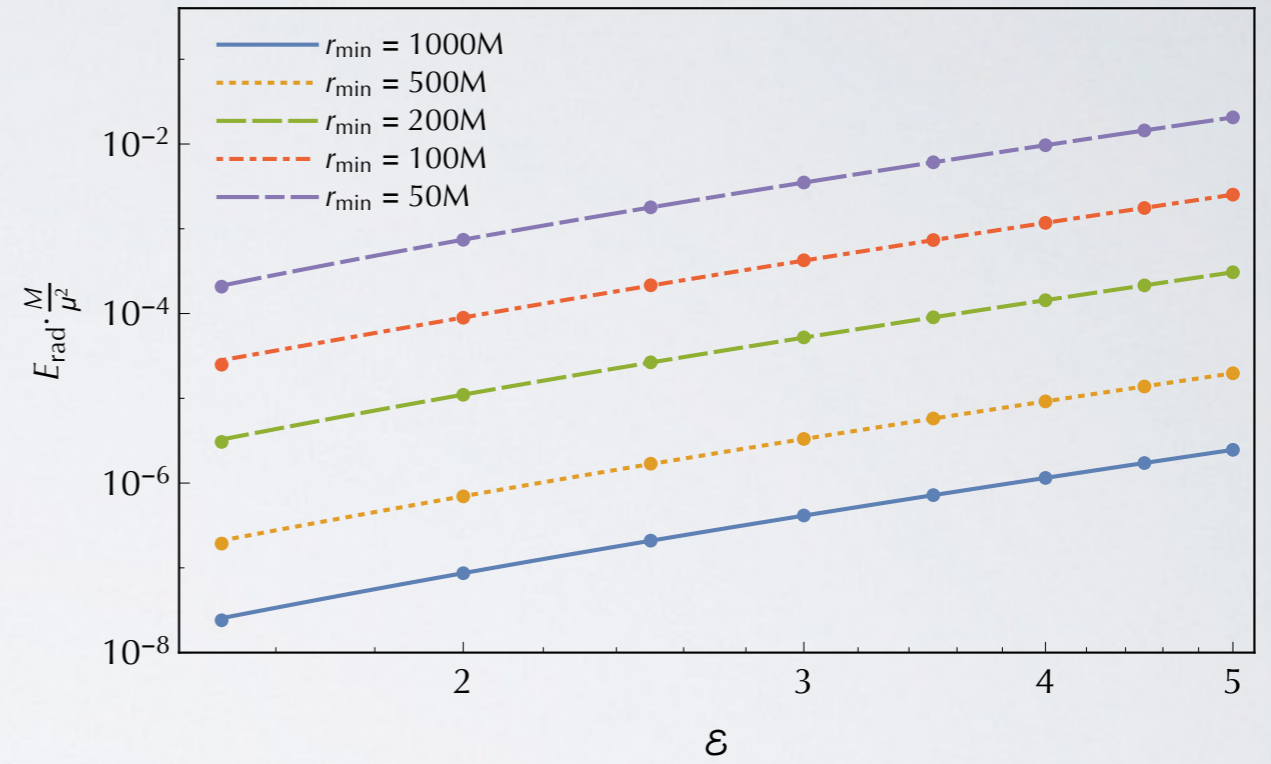


At high energies we agree with Peters' predictions



$v \ll c$

$$\frac{E_{\text{rad}}}{M} = \frac{37\pi}{15} \frac{G^3}{c^5} \left(\frac{\mu}{M}\right)^2 \frac{v}{(r_{\min}/M)^3}$$



$\epsilon \gg 1$

$$\frac{E_{\text{rad}}}{M} \sim \frac{G^3}{c^4} \left(\frac{\mu}{M}\right)^2 \frac{\epsilon^3}{(r_{\min}/M)^3}$$

28 ± 2

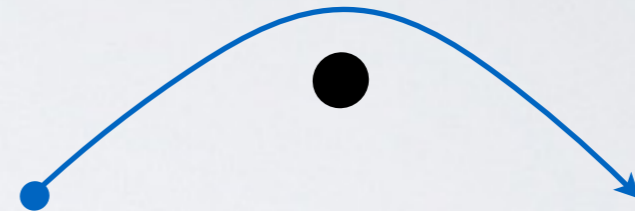


Outline

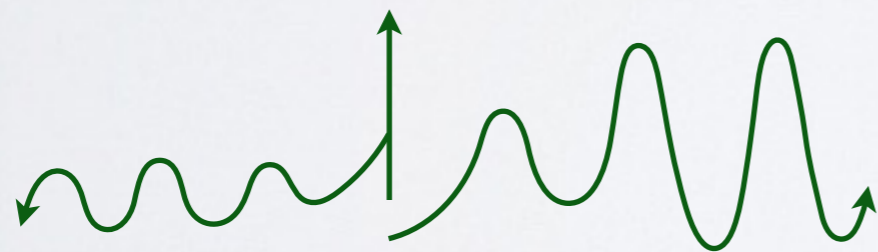
Bound motion



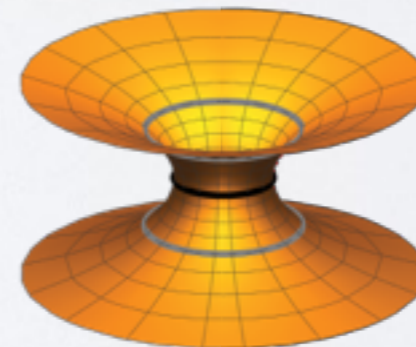
Unbound motion



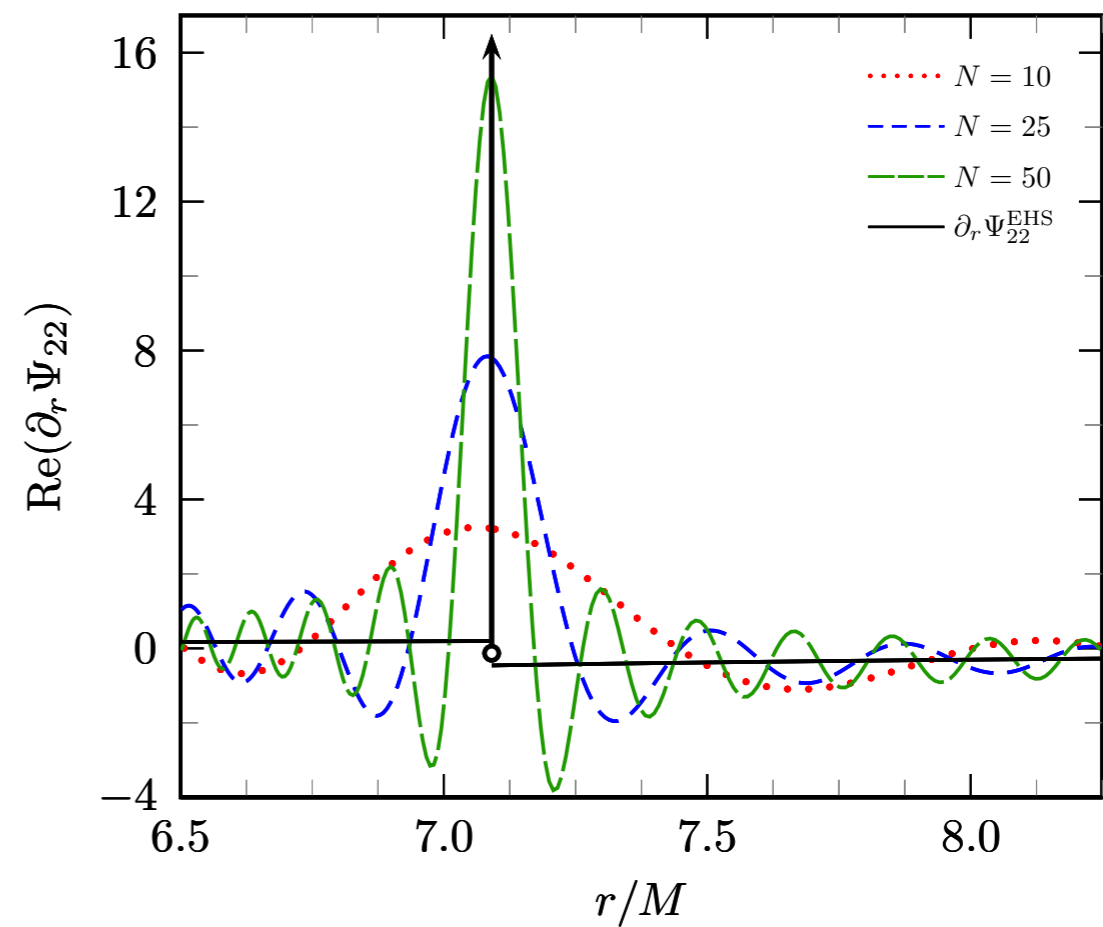
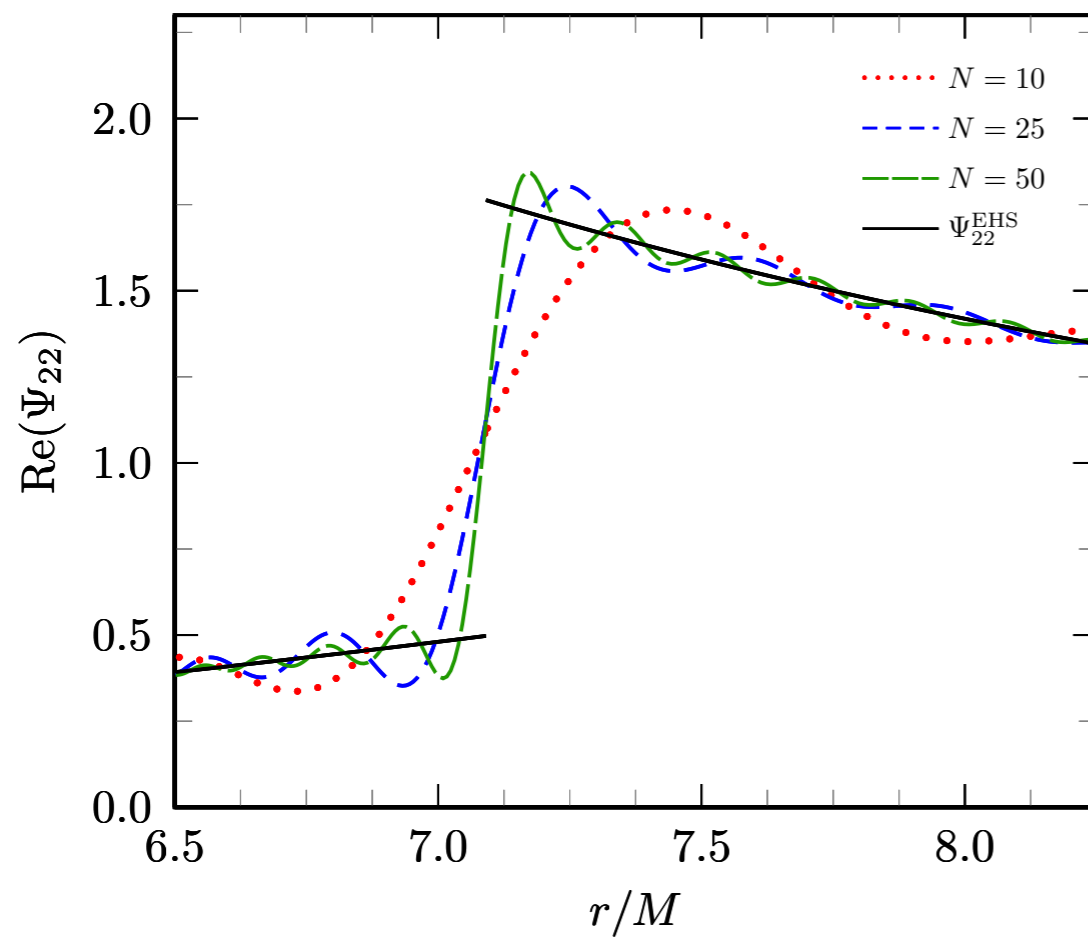
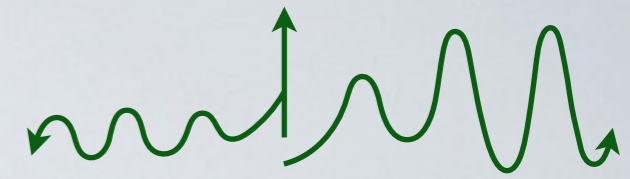
Local calculations



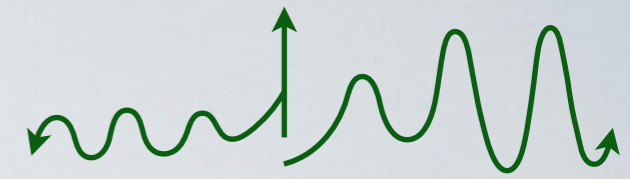
Wormholes and echoes



The point particle can cause a Gibbs phenomenon

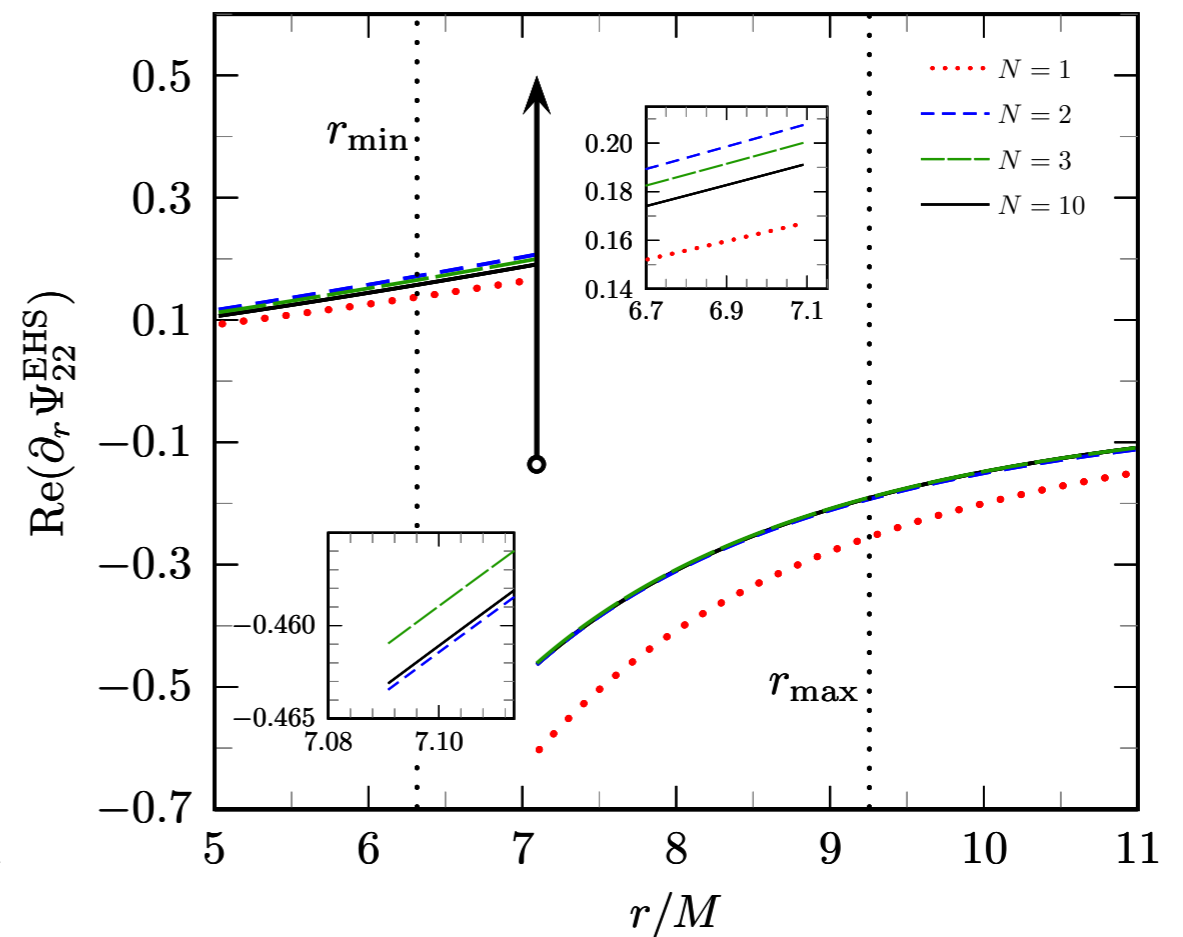
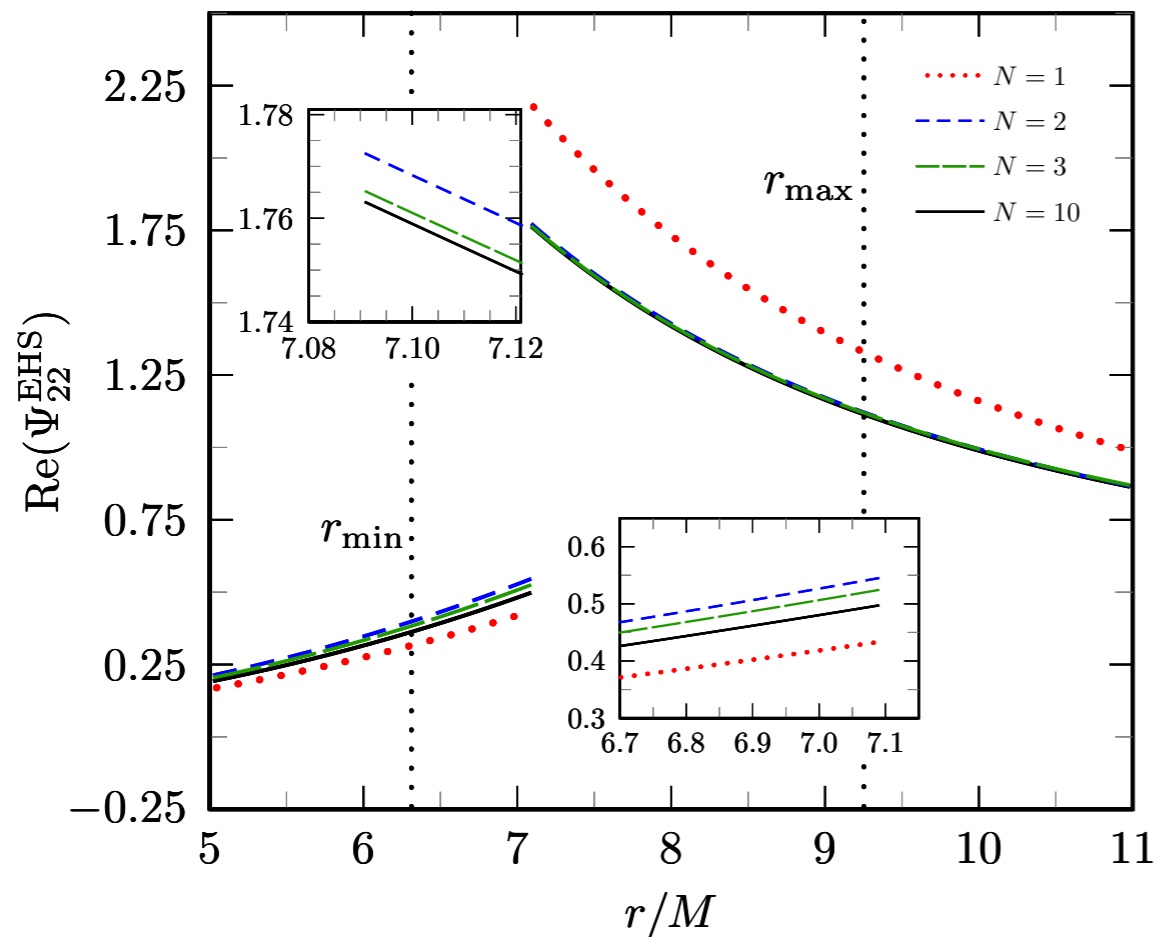


'Extended homogeneous solutions' avoids this problem

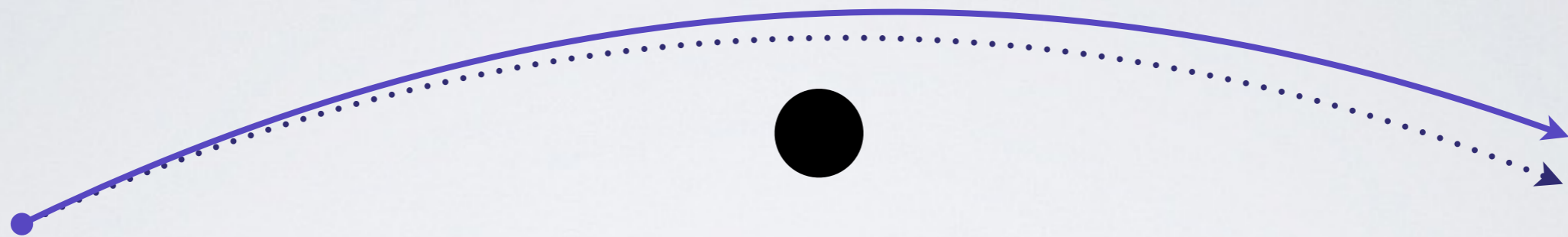
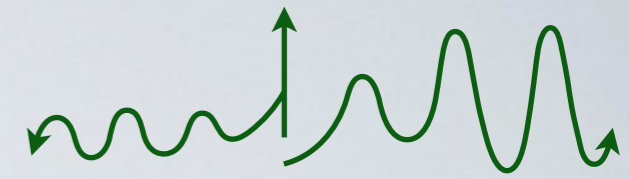


Barack, Ori, Sago

Hopper, Evans



Scatters also have gauge invariants



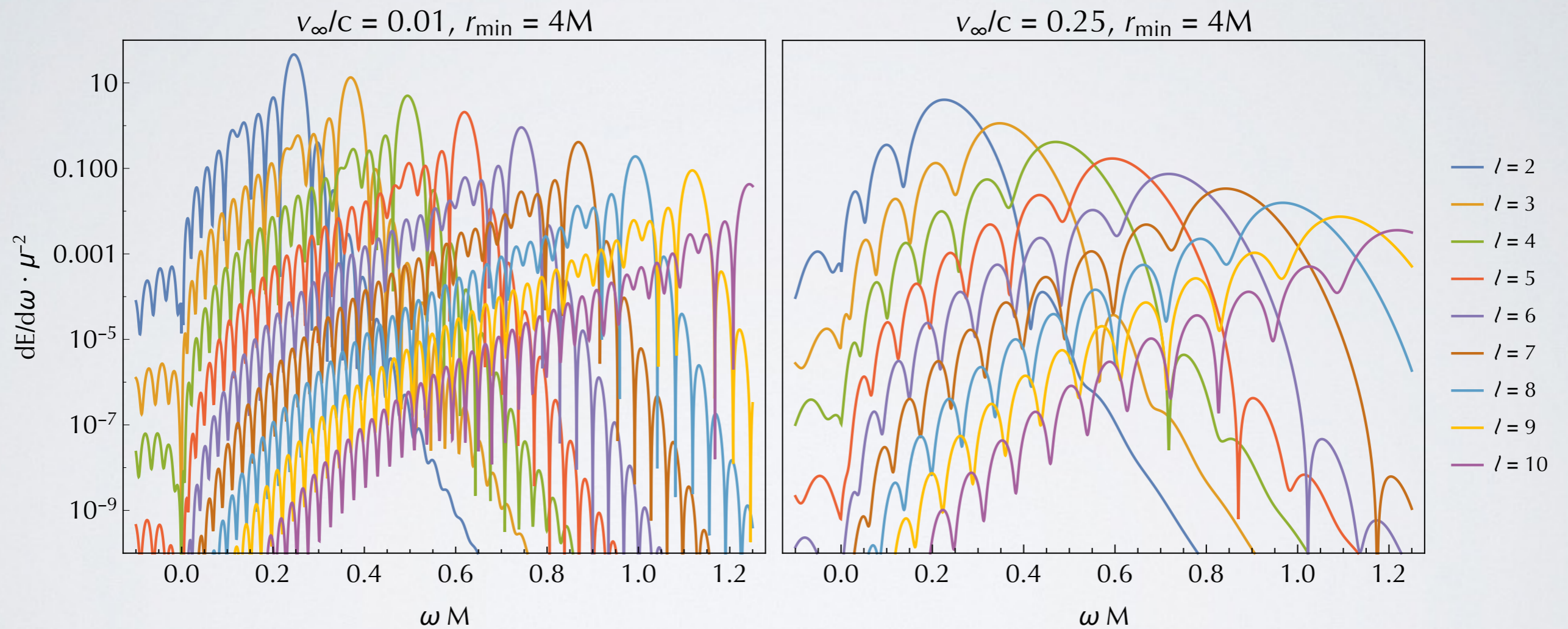
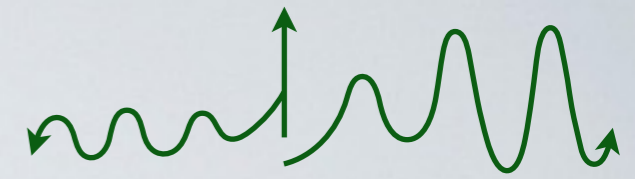
Generalized redshift:

$$\delta \left(\frac{T}{\mathcal{T}} \right)$$

Angle of deflection:

$$\delta (\Delta\theta)$$

Local calculations are hard, any way you cut it

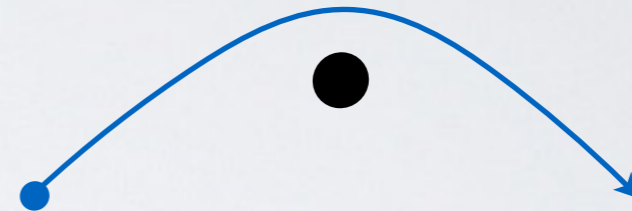


Outline

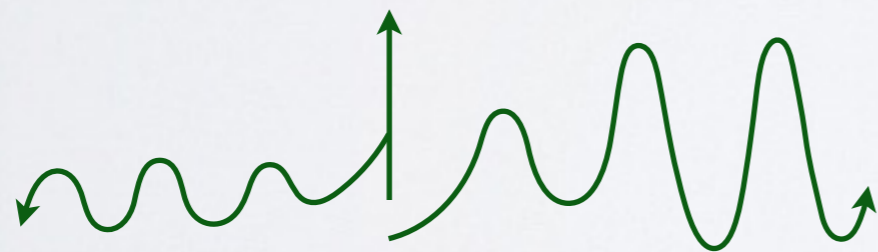
Bound motion



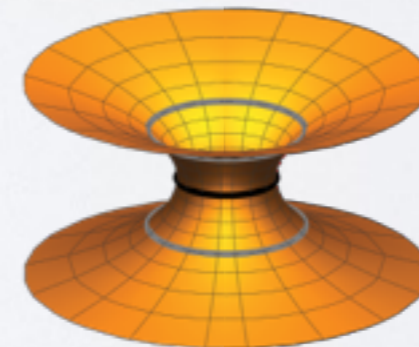
Unbound motion



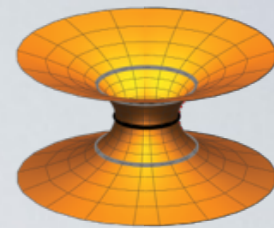
Local calculations



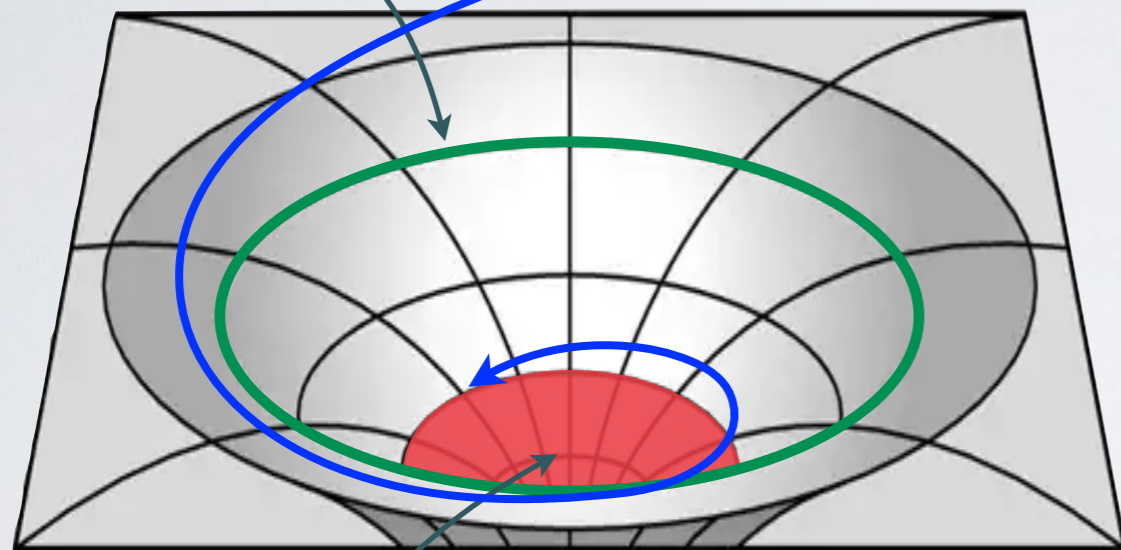
Wormholes and echoes



Black holes ring because they have “light rings”

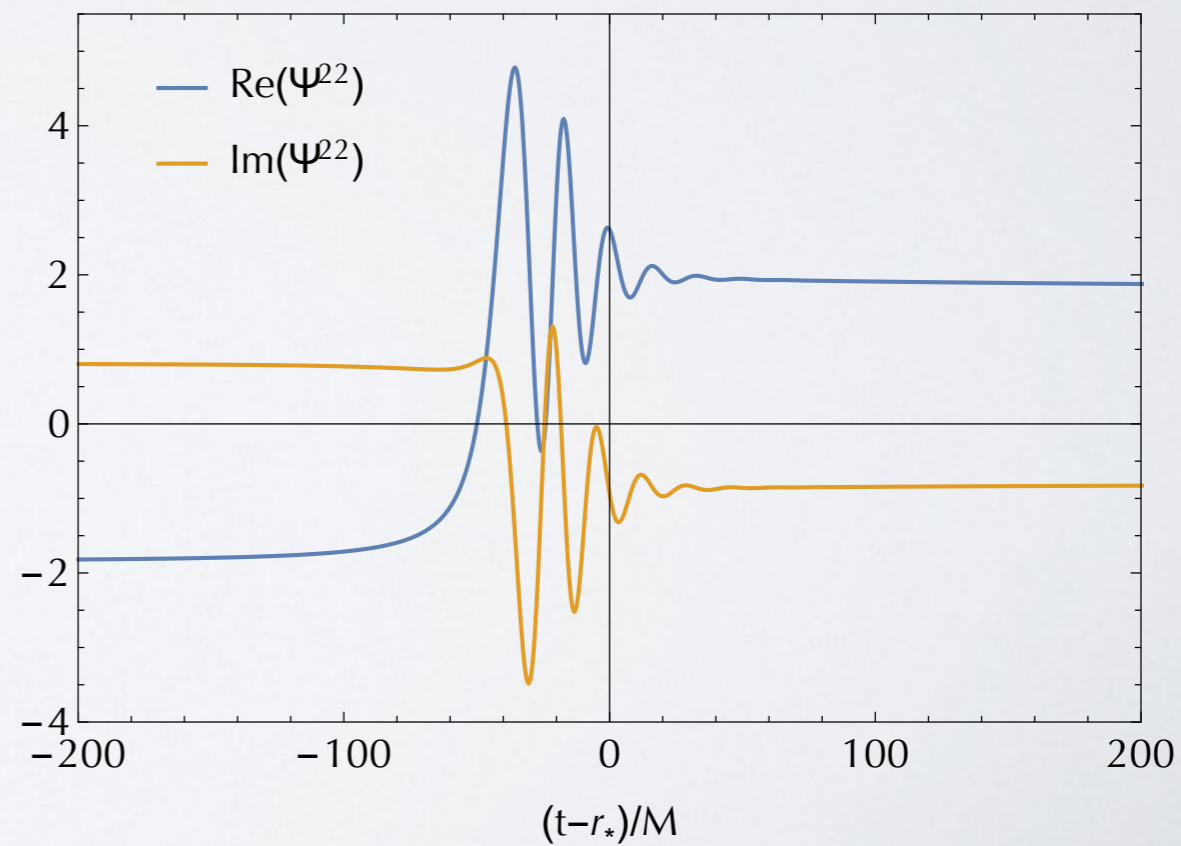


Light ring

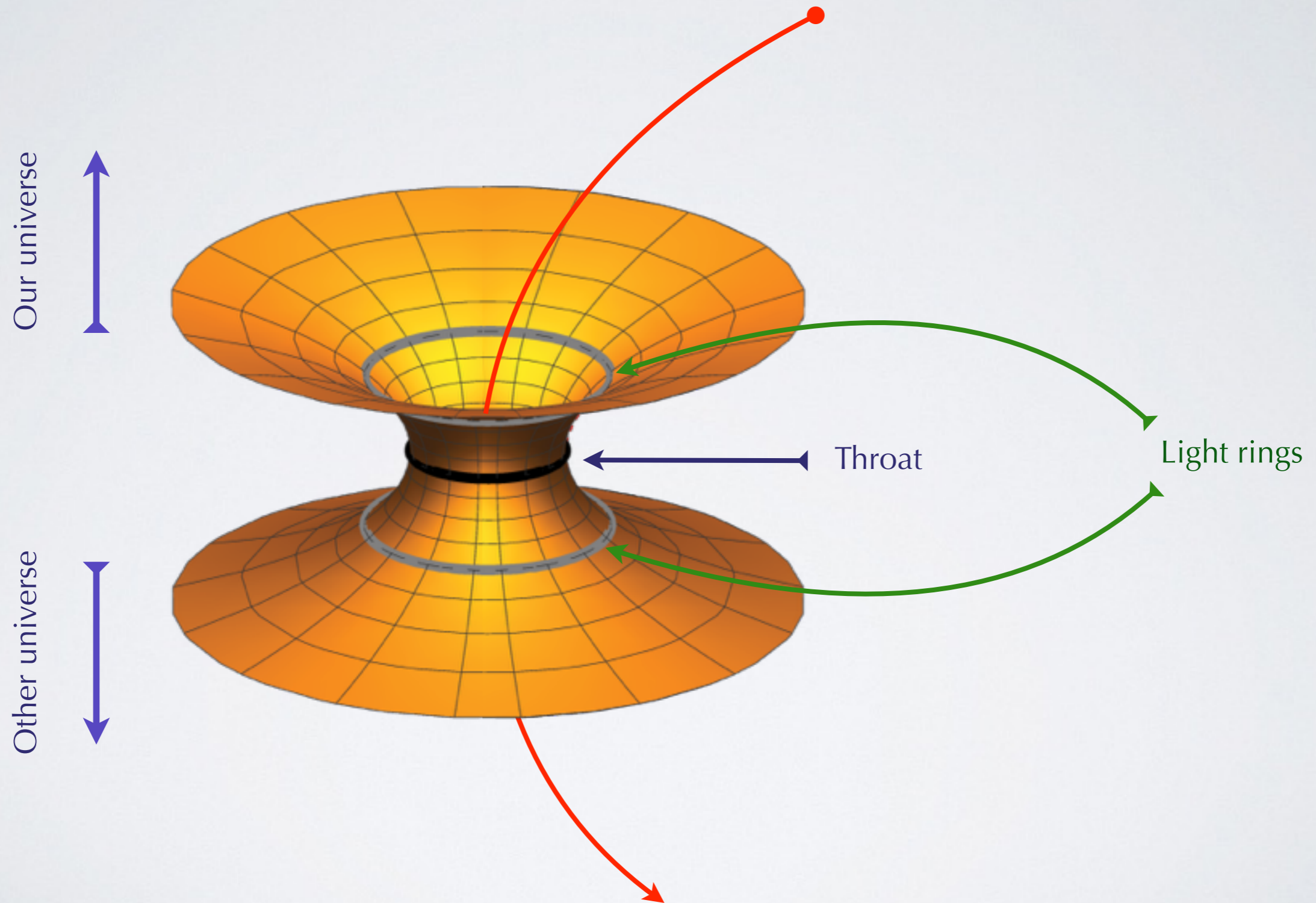
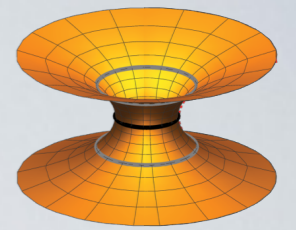


Event horizon

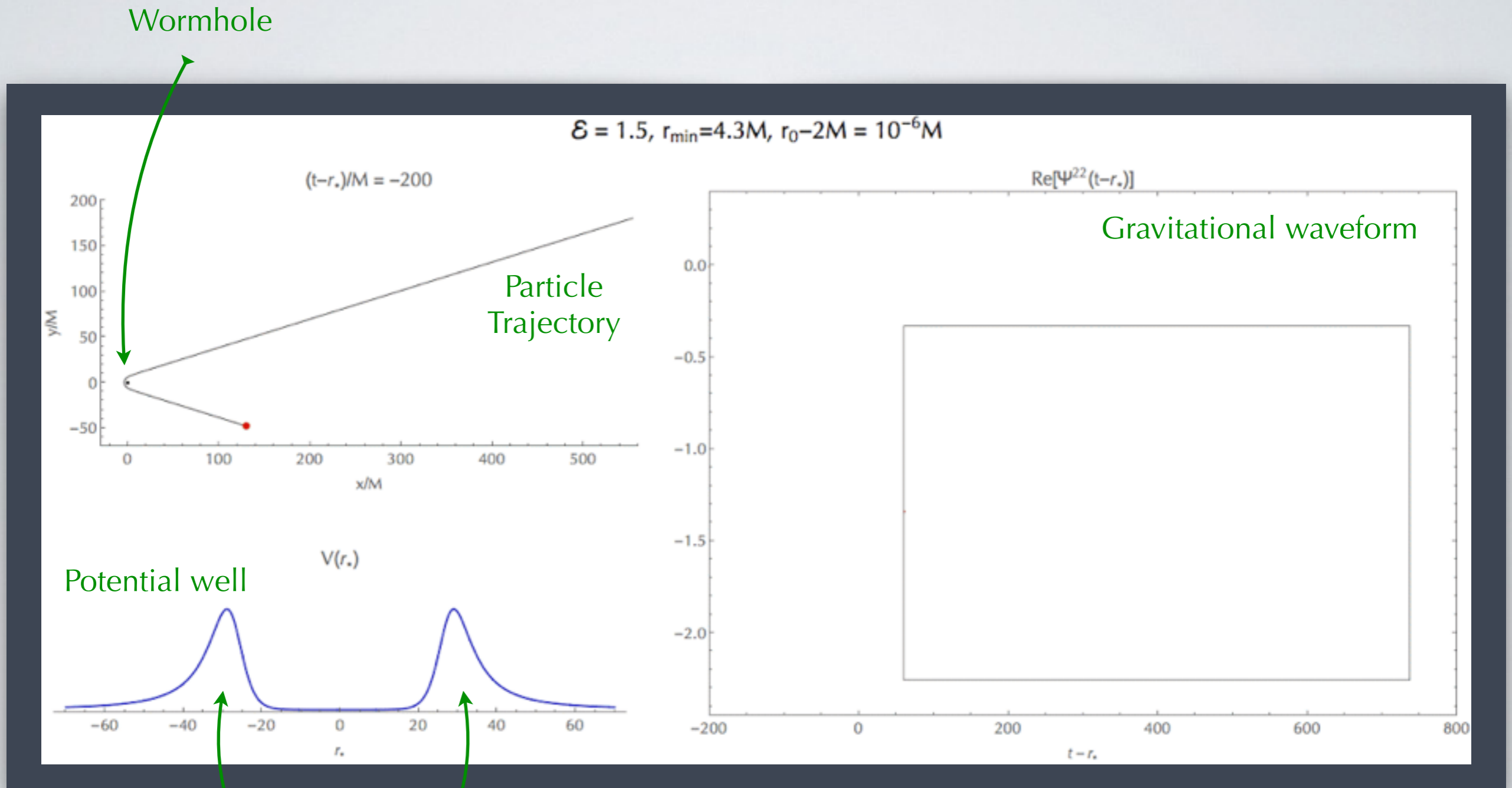
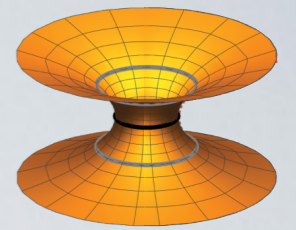
$\mathcal{E} = 3, \mathcal{L}/\mathcal{L}_{\text{crit}} = 0.99$



A wormhole can have two light rings



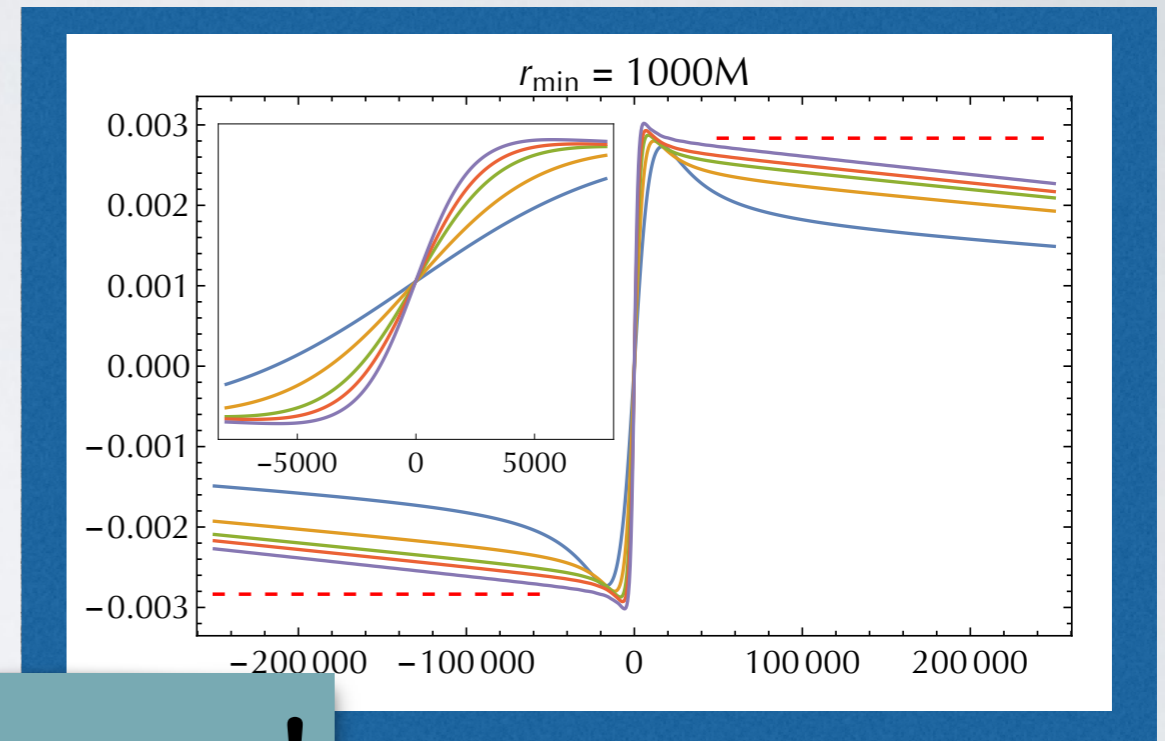
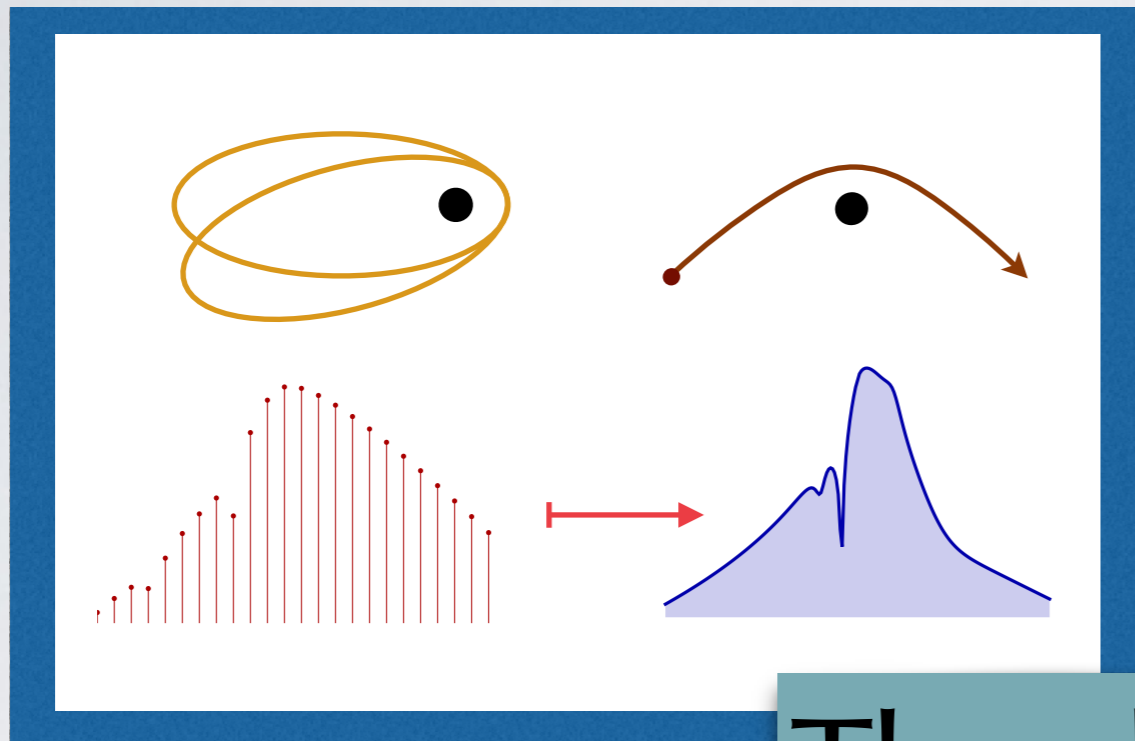
A wormhole rings like a black hole at first, but echoes later



Light rings

Cardoso, Hopper, Macedo, Palenzuela, Pani

These are the main points



Thank you!

